

# A Methodology of Cooperative Driving based on Microscopic Traffic Prediction

Boris S. Kerner<sup>1</sup>, Sergey L. Klenov<sup>2</sup>, Vincent Wiering<sup>1</sup>, and Michael Schreckenberg<sup>1</sup>

<sup>1</sup> *Physics of Transport and Traffic, University of Duisburg-Essen, 47048 Duisburg, Germany and*

<sup>2</sup> *Moscow Institute of Physics and Technology, Department of Physics, 141700 Dolgoprudny, Moscow Region, Russia*

We present a methodology of cooperative driving in vehicular traffic, in which for short-time traffic prediction rather than one of the statistical approaches of artificial intelligence (AI), we follow a qualitative different microscopic traffic prediction approach developed recently [Phys. Rev. E 106 (2022) 044307]. In the microscopic traffic prediction approach used for the planning of the subject vehicle trajectory, no learning algorithms of AI are applied; instead, microscopic traffic modeling based on the physics of vehicle motion is used. The presented methodology of cooperative driving is devoted to application cases in which microscopic traffic prediction without cooperative driving cannot lead to a successful vehicle control and trajectory planning. For the understanding of the physical features of the methodology of cooperative driving, a traffic city scenario has been numerically studied, in which a subject vehicle, which requires cooperative driving, is an automated vehicle. Based on microscopic traffic prediction, in the methodology first a cooperating vehicle(s) is found; then, motion requirements for the cooperating vehicle(s) and characteristics of automated vehicle control are predicted and used for vehicle motion; to update predicted characteristics of vehicle motion, calculations of the predictions of motion requirements for the cooperating vehicle and automated vehicle control are repeated for each next time instant at which new measured data for current microscopic traffic situation are available. With the use of microscopic traffic simulations, the evaluation of the applicability of this methodology is illustrated for a simple case of unsignalized city intersection, when the automated vehicle wants to turn right from a secondary road onto the priority road.

PACS numbers: 89.40.-a, 47.54.-r, 64.60.Cn, 05.65.+b

## I. INTRODUCTION

### A. Brief Overview of Approaches to Cooperative Driving

Cooperative driving is currently one of the most developing fields in physics of vehicular traffic. For the realization of cooperative driving, a vehicular networking is usually needed, i.e., a vehicular network in which vehicles can communicate to each other through vehicle-to-vehicle (V2V) communication or/and through vehicle-to-infrastructure communication; both types of vehicular communications are called V2X-communication (see, e.g., [1–5]). Through V2X-communication vehicles can have additional information about the behaviors of other vehicles.

In particular, it is assumed that cooperative driving should support the motion of automated-driving vehicles (automated vehicles for short) (see, e.g., [6–71]). The information obtained through V2X-communication can also be used for a short-time prediction of a traffic situation, for example, based on a so-called partially observable Markov decision process (see, e.g., [72–79]), learning algorithms (see, e.g., [80–102]) as well as many other artificial intelligence (AI) and model approaches (see, e.g., [103–124]). The short-time prediction of vehicle variables (vehicle locations and speeds) is required for the vehicle trajectory planning.

Thus, the short-time prediction of vehicle variables (vehicle locations and speeds), which is required for the vehicle trajectory planning, is usually made based on a di-

verse variety of *statistical* approaches of AI. Some of these statistical approaches have been mentioned above [72–124].

For reasons that will be explained in Sec. VI B, rather than one of the statistical approaches of AI, in this paper we follow a qualitative different approach, which is based on the physics of vehicle motion in vehicular traffic. In this approach introduced in [125], *no* statistical analysis of a historical traffic database is used for traffic prediction. Instead of statistical analysis of empirical traffic data, microscopic traffic modeling with a traffic flow model that can reproduce spatiotemporal features of real traffic is applied. Based on this microscopic traffic modeling, the microscopic short-time prediction of vehicle variables (vehicle locations and speeds) is made. This prediction is used for the planning of the vehicle trajectory. Because the microscopic traffic prediction of [125] is the scientific basis of the methodology of cooperative driving presented in this paper, for the paper understanding we present a brief summary of this microscopic traffic prediction approach below.

### B. Brief Summary of Microscopic Traffic Prediction

General features of the microscopic traffic prediction approach of [125] are as follows:

- (i) We assume that through vehicular networking (in particular, V2X-communication) at some time in-

stants

$$t = t_p, p = 1, 2, 3, \dots \quad (1)$$

locations (including the correspondence to road lanes) and speeds of all vehicles moving around of a subject vehicle are known. We call the multitude of the vehicle locations  $x$  and vehicle speeds  $v$  as a *microscopic traffic situation* at time instant  $t_p$ . In general, a time interval  $\delta t = t_{p+1} - t_p$ ,  $p = 1, 2, 3, \dots$  that can be very short (e.g., between 0.1 s and 1 s) should not be necessarily a constant value; this time interval is determined by the measurement technology of the microscopic traffic situation. However, for simulations made in [125] as well as in this paper we apply a constant time interval

$$\delta t = t_{p+1} - t_p = \tau, p = 1, 2, 3, \dots \quad (2)$$

where  $\tau$  is a time-independent time step of the model used for microscopic simulations (in all simulations we use  $\tau = 1$  s).

- (ii) A microscopic traffic situation measured at time instant  $t = t_p$ , i.e., values for locations and speeds of vehicles related to  $t = t_p$  are set into the prediction model. These locations and speeds of vehicles are used as an initial condition for a microscopic traffic flow model of vehicular traffic. For this time instant  $t = t_p$ , the microscopic traffic flow model calculates future (predicted) microscopic traffic situation that the model predicts for prediction horizon  $\Delta T_p$ .
- (iii) Based on this microscopic prediction, parameters of control of the subject vehicle applied at time instant  $t = t_p$  are calculated. The automated vehicle control application should ensure a safety planning of the subject vehicle trajectory based on calculated control parameters.
- (iv) It should be emphasized that the real application of the calculated control parameters for the safety planning of the subject vehicle trajectory at time instant  $t = t_p$  (1) is only possible if a microscopic traffic model used for the microscopic prediction during the prediction horizon  $\Delta T_p$ ,  $p = 1, 2, 3, \dots$  can make the related calculation during a negligible short time interval in comparison with time interval (2). This is because only in this case the microscopic traffic prediction remains to be a current one for the calculations of subject vehicle control used for the safety planning of the subject vehicle trajectory at time instant  $t = t_p$ . Note that the time-discrete traffic flow model for traffic of [125] used in the paper (see Sec. IC) is able to perform such calculations during a negligible short time interval in comparison with time interval (2).
- (v) The subject vehicle moves in accordance with calculated control parameters only during the time interval

$$t_p \leq t < t_{p+1}, p = 1, 2, 3, \dots \quad (3)$$

Indeed in accordance with item (i), at  $t = t_{p+1}$  a new measured microscopic traffic situation is available. Therefore, both the microscopic traffic prediction and resulting parameters of subject vehicle control made for time instant  $t = t_p$  become obsolete.

- (vi) For this reason, at  $t = t_{p+1}$  the measured microscopic traffic situation is used as a new initial condition for microscopic traffic prediction during prediction horizon  $\Delta T_{p+1}$ . The prediction is used for the calculation of new parameters of subject traffic control used at  $t = t_{p+1}$ . The parameters of subject traffic control are applied only during time interval  $t_{p+1} \leq t < t_{p+2}$ . Then, at  $t = t_{p+2}$  a new measured microscopic traffic situation is used as a new initial condition for microscopic traffic prediction during prediction horizon  $\Delta T_{p+2}$ ; the microscopic prediction is used for the calculation of new parameters of subject traffic control used at  $t = t_{p+2}$ , which are applied only during time interval  $t_{p+2} \leq t < t_{p+3}$ , and so on.
- (vii) Thus in the microscopic prediction approach, both the microscopic traffic prediction and the resulting calculation of parameters for subject vehicle control are repeated for each new time instant (1), whereas the control parameters are used only during the related time interval (3) before a new measured microscopic traffic situation is available.
- (viii) The microscopic traffic prediction approach introduced in [125] (see footnote [84] of [125]) is a general approach because it is applicable for both the control of automated-driving and human-driving vehicles. For this reason, the vehicle for which the microscopic traffic prediction approach is applied has been called above as the subject vehicle. In [125], we have illustrated this general microscopic traffic prediction approach for the trajectory planning of the subject vehicle that is an automated vehicle. Indeed, the trajectory planning of automated vehicles is currently one of the priority aims in traffic science.

With the use of Fig. 1, we make a brief explanation of one of the applications of the general features of microscopic traffic prediction approach (items (i)–(viii) above). We assume that an automated vehicle moving on a secondary road wants to turn right on the priority road at a unsignalized city intersection (Fig. 1(a)). The basic objective of the microscopic traffic prediction approach is to predict time dependencies of locations and speeds of vehicles in a vicinity of the interaction that allow us to control the motion of automated vehicle. The objective of this automated vehicle control is to make possible the turning right of the automated vehicle without the stopping at the intersection. In this case, the parameter of automated vehicle control for the planning of automated vehicle trajectory is deceleration/acceleration of

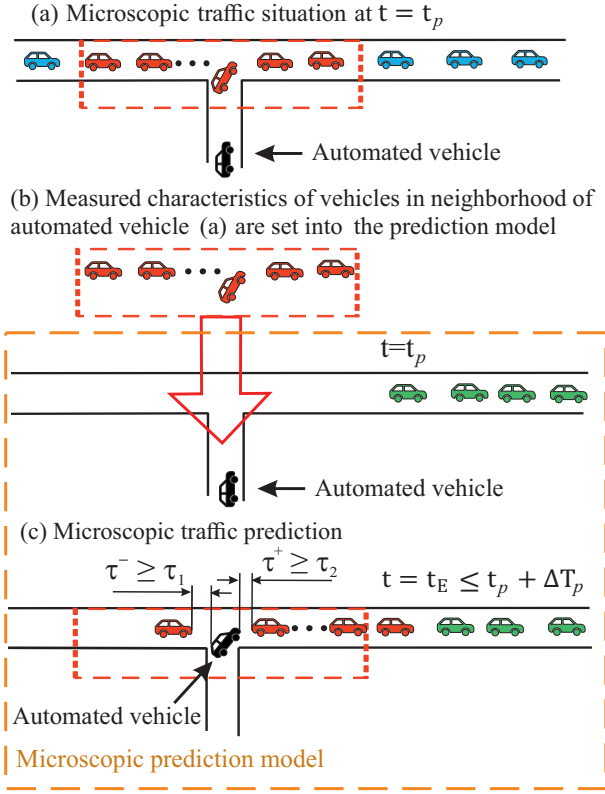


FIG. 1: Qualitative schema of microscopic traffic prediction for an unsignalized intersection: (a) Microscopic traffic situation measured at  $t = t_p$  (1); only red colored vehicles that are in a red colored dashed road region can affect on the motion of the automated vehicle (black colored vehicle). (b) The measured characteristics of red colored vehicles (vehicle speeds, vehicle locations, vehicle lengths, and so on) in the red colored dashed road region shown in (a) are used in the microscopic prediction model; before, all vehicles that were at  $t < t_p$  in this dashed road region of the microscopic prediction model are removed. (c) Through the use of the microscopic traffic prediction, a predicted time instant  $t_E$  is found at which the vehicle should turn right onto the priority road. Adapted from [125].

the automated vehicle while the vehicle approaches the intersection.

For the application scenario under consideration (Fig. 1), the calculation of the microscopic traffic prediction begins at some  $t = t_p = t_1$  (i.e., at  $p = 1$ ) at which a vehicle that is the preceding vehicle for the automated vehicle has just left the secondary road while turning right on the priority road. In this case, at  $t = t_1$  control of automated vehicle can be made based on prediction of locations and speeds of vehicles moving only on the priority road (this case is shown in Fig. 1(a)).

For each of the given time instant  $t_p$ ,  $p = 1, 2, 3, \dots$ , in addition to the microscopic traffic prediction, the prediction model calculates two predicted time instants:  $t = t_{\min}$  and  $t = t_{\max}$ . The physical sense of these predicted time instants is as follows:  $t_{\min}$  and  $t_{\max}$  are pre-

dicted time instants at which the automated vehicle can reach the intersection moving, respectively, with maximum acceleration (or/and maximum speed) and with a safe speed coming to a stop at  $t = t_{\max}$ .

With the use of  $t = t_{\min}$  and  $t = t_{\max}$ , the prediction model searches whether there is a pair of vehicles moving on the priority road between which the automated vehicle can merge without stopping at the intersection while satisfying some given safety conditions. In this case

$$t_{\min} \leq t_E < t_{\max}, \quad (4)$$

where  $t = t_E$  is a predicted time instant at which the automated vehicle can safety turn right at the intersection between the above-mentioned pair of vehicles moving on the priority road;  $t_{\min}, t_E, t_{\max} > t_1$ .

In microscopic traffic prediction made at each time instant  $t_p$ , the safety conditions at which a pair of vehicles moving on the priority road between which the automated vehicle can merge without a stop at the intersection are as follows:

$$\tau^- \geq \tau_1, \quad \tau^+ \geq \tau_2, \quad (5)$$

in which

$$\tau^- = (s^- - d)/v^-, \quad \tau^+ = (s^+ - d)/v^{(AV)}, \quad (6)$$

where  $s^+$  is a gross space gap between the automated vehicle and the preceding vehicle;  $s^-$  is a gross space gap between the automated vehicle and the following vehicle;  $v^-$  is the speed of the following vehicle;  $v^{(AV)}$  is the speed of the automated vehicle; all values in (6) are related to a predicted time instant  $t = t_E$  at which the automated vehicle could turn right at the intersection. In (5),  $\tau^-$  is time headway of a vehicle following the automated vehicle on the priority road just after the merging,  $\tau^+$  is time headway of the automated vehicle to the preceding vehicle on the priority road just after the merging,  $\tau_1$  and  $\tau_2$  are model parameters. The predicted time instant  $t = t_E$ , at which the automated vehicle can merge without a stop at the intersection, in addition to safety conditions (5), should satisfy conditions (4).

Such a case, when safety conditions (5) are satisfied, is shown in Fig. 1(c). Only in this case, predicted time instant  $t = t_E$  is used for the calculation of automated vehicle deceleration. Otherwise, when at least one of the safety conditions (5) is not satisfied, the automated vehicle stops at the intersection.

The predicted time instant  $t = t_E$  is used for the calculation of automated vehicle deceleration that is applied at  $t = t_1$ . In accordance with item (v) of the general approach to microscopic traffic prediction, the automated vehicle moves in accordance with calculated deceleration only during the time interval  $t_1 \leq t < t_2$ . At time instant  $t = t_2$ , a new measured microscopic traffic situation is available. Therefore, a new microscopic traffic prediction is calculated at which new predicted time instants  $t_{\min}$ ,  $t_{\max}$ , and  $t_E$  as well as a new vehicle deceleration are found. The automated vehicle moves in accordance

with deceleration calculated at time instant  $t = t_2$  only during the time interval  $t_2 \leq t < t_3$ . At time instant  $t = t_3$ , a new measured microscopic traffic situation is available, new predicted time instants  $t_{\min}$ ,  $t_{\max}$ , and  $t_E$  as well as a new vehicle deceleration are found, and so on. After the automated vehicle has turned right, the automated vehicle moves on the priority road in accordance with given rules of automated vehicle motion.

### C. About Mathematical Model used for Simulations of Cooperative Driving

Mathematical formulations of [125] that are used for simulations of cooperative driving in the paper are as follows: We use the same microscopic model of mixed traffic flow as that considered in Secs. II C of [125]. Model for simulations of microscopic traffic situation has been considered in Secs. II D of [125]. Model of motion of human-driving vehicles has been given in Appendix A of [125]. Models of the vehicle merging onto the priority road for human-driving vehicles and for automated vehicles (when the microscopic traffic prediction is not used) have been given in Appendix B of [125]. Model for simulations of microscopic traffic prediction has been taken from Sec. III and Appendix C of [125].

It should be noted that there are a huge number of other different microscopic traffic flow models for mixed traffic (see, e.g., [126–139])[149]. A basic requirement to a model for simulations of the microscopic traffic prediction is that the model of human-driving vehicles should simulate microscopic behavior of human drivers in different traffic situations as close as possible to real measured traffic data. For motion of human-driving vehicles in mixed traffic, we use a version of a microscopic stochastic time-discrete model of Kerner and Klenov in the framework of three-phase traffic theory (see Appendix A in [140]); in the model, in addition to hypotheses of the three-phase traffic theory, well-known slow-to-start rule [141, 142], and Gipps' formulation for safe speed [143–145] have been used; contrary to Appendix A in [140], the successive number of time steps of the delay in acceleration of a human-driving vehicle has been limited as made in [125] (see formulas (A17) and (A18) of Appendix A of [125]). The use of this model for human-driving vehicles is explained as follows: as proven in [140], the Kerner-Klenov model satisfies the above-mentioned basic requirement following from empirical features of real traffic. In the traffic model, update rules of motion of automated driving vehicles are simulated with a time-discrete version of the classical ACC model (e.g., [6–11]) that is equivalent to Helly's model [146].

The time-discrete traffic flow model of [125] used in this paper for simulations calculates a new microscopic traffic prediction (see items (ii) and (vi) of Sec. IB) for the motion of about 30 vehicles during a time interval  $\theta < 0.005$  s, which is negligible short in comparison with time interval  $\delta t = t_{p+1} - t_p = \tau = 1$  s (2).

### D. Objective, Focus, and Organization

The *objective* of this paper is the presentation of a methodology for cooperative driving vehicular traffic based on short-time microscopic traffic prediction of [125]. It must be emphasized that contrary to the analysis of applications of microscopic traffic prediction made in [125], the methodology of cooperative driving presented in this paper is devoted to application cases in which microscopic traffic prediction without the use of cooperative driving *cannot* lead to a successful vehicle control and trajectory planning. In other words, the objective of the paper under consideration makes sense only then, if subject vehicle motion control based on the microscopic traffic prediction without cooperative driving *does not* lead to the merging of the subject vehicle onto the priority road without stopping at the intersection. For this reason, the methodology of cooperative driving based on the microscopic traffic prediction (Sec. II), the physics and the procedure of calculations of cooperative driving (Sec. IV) and results of simulations of this cooperative driving (Sec. V) are qualitatively different from results of [125] in which no cooperative driving has been assumed. We limit our analysis of this methodology of cooperative driving based on microscopic traffic prediction by a case vehicular traffic in which 100% of vehicles can participate and are willing to participate in cooperative driving.

The main *focus* of this paper is the presentation of a general methodology for cooperative driving based on microscopic traffic prediction. To study the physical features of this general methodology for cooperative driving, we limit simulations by the same simple case of unsignalized city intersection discussed in [125] (Fig. 1) in which a subject vehicle is the automated vehicle that tries to turn right from the secondary road onto the priority road without stopping at the intersection. Contrary to the case shown qualitatively in Fig. 1 and explained above in Sec. IB, we simulate a traffic scenario at which microscopic traffic prediction cannot be used for the safety vehicle merging without the vehicle stopping at the intersection.

The paper is organized as follows: The general methodology of cooperative driving based on the microscopic traffic prediction is presented in Sec. II. A simple scenario of cooperative driving for simulations of the general methodology is discussed in Sec. III. The physics of calculations of cooperative driving has been studied in Sec. IV. Results of simulations of this cooperative driving are presented in Sec. V. In discussion section (Sec. VI), we consider limitations of cooperative driving (Sec. VIA), briefly compare applications of leaning algorithms for traffic prediction versus microscopic traffic prediction based on the physics of vehicle motion used in the paper (Sec. VIB), discuss other possible applications of the general methodology of cooperative driving (Sec. VIC), consider the effect of data uncertainty on prediction reliability (Sec. VID) as well as formulate

conclusions of the paper (Sec. VIE).

## II. METHODOLOGY OF PHYSICAL MODELING OF COOPERATIVE DRIVING IN VEHICULAR TRAFFIC

The general methodology for cooperative driving presented here can be applied for both automated-driving and human-driving vehicles. In this case, as mentioned above (see item (viii) of Sec. IB), a vehicle, which uses the cooperative driving, can be called as a subject vehicle, to distinguish the vehicle from cooperating vehicles. However, the trajectory planning of automated vehicles is one of the priority aims in traffic science. For this reason, in the paper we have limited the study of the physics of the general methodology of cooperative driving for a case in which the subject vehicle is the automated vehicle.

The general methodology of physical modeling of cooperative driving is as follows.

- (i) First, microscopic traffic prediction [125] for the subject vehicle control without the application of cooperative driving is made, as briefly explained in Sec. IB.

Contrary to [125], in this paper we consider microscopic traffic situations for which already at

$$t_p = t_1 \quad (7)$$

the calculated microscopic traffic prediction shows that no effective subject vehicle control is possible. Therefore, to organize the effective subject vehicle control, a cooperative driving based on microscopic traffic prediction is applied for subject vehicle control. At  $t_p = t_1$  (7), the following stages (ii) and (iii) of cooperative driving based on microscopic traffic prediction are applied.

- (ii) Based on the calculated microscopic traffic prediction considered in Sec. IB, between vehicles that are willing to cooperate vehicles that are suitable ones for the realization of cooperative driving are found. These vehicle are called below as “cooperating vehicles”.
- (iii) Microscopic traffic prediction found at  $t_p = t_1$  (Sec. IB) is further used to find both motion requirements for the cooperating vehicles and related characteristics of subject vehicle control. The prediction of the vehicle locations and vehicle speeds are used for the calculation of the future trajectory of the subject vehicle as well as all other vehicles involved in cooperative driving.

The microscopic traffic prediction together with the determination of the cooperating vehicles as well as the associated calculation of motion requirements for the cooperating vehicles and characteristics of subject vehicle control are only possible when the

microscopic model is able to calculate all these characteristics during negligible short time interval in comparison with time interval  $\delta t = t_{p+1} - t_p$ . It should be emphasized that as explained in Sec. IB the time-discrete traffic flow model for mixed traffic of [125] used in this paper is able to perform these calculations during a negligible short time interval.

- (iv) Stages (ii) and (iii) explained above are repeated at the next time instant  $t_{p+1}$ ,  $p = 1, 2, 3, \dots$ , when a next microscopic traffic situation is known. The new microscopic traffic situation is used as an initial condition for the microscopic traffic flow model. Then, the model makes the microscopic traffic prediction for vehicle locations and vehicle speeds during prediction horizon  $\Delta T_{p+1}$  (prediction horizon  $\Delta T_p$  can be different for different time instants  $t_p$ ). Stages (ii) and (iii) are iterated for each new time instants, and so on, once data for new microscopic traffic situations are available.

Thus, as in [125] (Sec. IB), in the methodology for cooperative driving there is the repetition of the microscopic traffic prediction together with the calculation of motion requirements for the cooperating vehicle for any current time instant  $t_p$  (1) at which microscopic traffic situations are available. This allows us to update the calculations of the trajectories of both the cooperating vehicles and the subject vehicle during the vehicle motion in traffic flow.

## III. APPLICATION SCENARIO OF COOPERATIVE DRIVING FOR UNSIGNALIZED INTERSECTION IN CITY TRAFFIC

In the paper, we study physical features of the above methodology of cooperative driving through numerical simulations of a common case in city traffic in which the subject vehicle is an automated vehicle. The automated vehicle (black colored vehicle “automated vehicle” in Fig. 2) moves initially on a secondary road and it would like to turn right onto a priority road. There is no traffic signal on the intersection of these two roads. The objective of cooperative driving is to find whether there is a possibility for the merging of the automated vehicle onto the priority road *without stopping* at the intersection.

As mentioned, the use of cooperative driving makes sense, if automated vehicle motion control based on the microscopic traffic prediction without cooperative driving does not lead to the merging of the automated vehicle onto the priority road without stopping at the intersection. Such a case is qualitatively shown in Fig. 2. Indeed, when the microscopic traffic prediction is applied for automated vehicle control, we can see in Fig. 2(b) that  $\tau^- < \tau_1$ , i.e., the first of safety conditions (5) is satisfied for none of the pairs of vehicles moving on the priority road during time interval  $t_{\min} \leq t < t_{\max}$ . This means

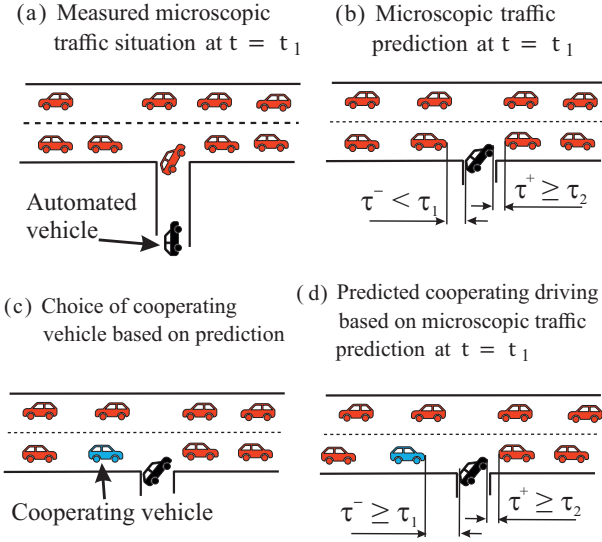


FIG. 2: Qualitative explanation of the methodology for cooperative driving based on microscopic traffic prediction.

that the automated vehicle must stop at the intersection.

To simulate the scenario qualitatively shown in Fig. 2, in accordance with item (i) of the general methodology of cooperative driving (Sec. II), the microscopic traffic prediction, in which no cooperative driving has been used, is made (Fig. 3). Simulations of the predicted time instants  $t_{\min}$  and  $t_{\max}$ , whose physical sense has been explained in Sec. IB, is shown in Fig. 4. In the simulations, in safety conditions (5) we have used  $\tau_1 = 2.0$  s and  $\tau_2 = 0.5$  s. It turns out that indeed already at the beginning of traffic prediction at  $t_p = t_1 = 148$  s condition  $\tau^- \geq \tau_1$  is satisfied for none of the pairs of vehicles moving on the priority road during time interval  $t_{\min} \leq t < t_{\max}$ . For this reason, the automated vehicle stops at the intersection (Fig. 3(b)). Only at some time instant  $t > t_{\max}$ , safety conditions (5) are satisfied and, therefore, the automated vehicle can merge onto the priority road (Fig. 3(a)).

Time instant  $t_p = t_1$  of the beginning of the prediction in the simulated scenario (Fig. 3) is  $t_1 = 148$  s (vertical red line  $t_1$  in Fig. 3). This is because at this time instant the preceding vehicle for the automated vehicle on the secondary road labeled by “i” (Fig. 3) has merged onto the priority road[150]. Thus, the following automated vehicle (black curves labeled by “automated vehicle” in Fig. 3) can choose its deceleration freely while approaching the intersection.

The result of these calculations of microscopic traffic prediction made for  $t_p = t_1 = 148$  s (Fig. 3) shows that in the scenario there are no pair of vehicles moving on the priority road for which *both* safety conditions (5) *and* conditions (4) for the merging of the automated vehicle without a stop at the intersection are satisfied. Therefore, the automated vehicle must stop at the intersection and wait as long as a pair of vehicles appears, which satisfying safety conditions (5), between which the automated

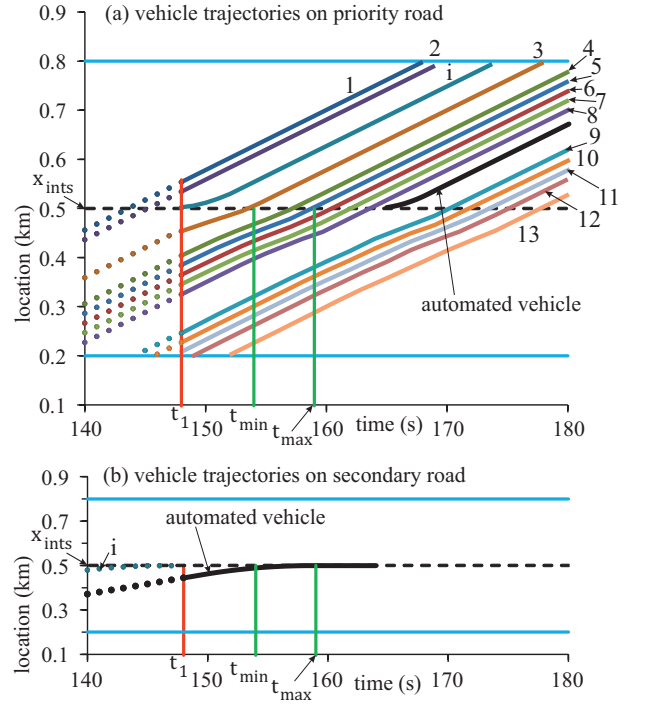


FIG. 3: Simulations of microscopic traffic prediction of automated vehicle motion with approach of [125] without the use of cooperative driving at  $t_p = t_1 = 148$  s: Vehicle trajectories on the priority road (a) and secondary road (b); dotted curves are vehicle locations of simulated microscopic traffic situations, solid curves are trajectories of the predicted vehicle trajectories. Parameters of the model of human driving vehicles are given in Table I of Appendix A of [125]; in (5),  $\tau_1 = 2.0$  s and  $\tau_2 = 0.5$  s; in model of the automated vehicle (see formulas (7)–(11) in Sec. II of [125]), we have used  $\tau_d^{(AV)} = 1.5$  s,  $K_1 = 0.3$  s $^{-2}$  and  $K_2 = 0.6$  s $^{-1}$ ,  $a_{\max}^{(AV)} = 2.5$  and  $b_{\max}^{(AV)} = 3$  m/s $^2$ , all other parameters of the model of the automated vehicle are the same as those in [125]. Results of calculations:  $t_{\min} = 154$  s and  $t_{\max} = 159$  s. A single-lane priority road is 2.5 km long; the intersection of this road with a single-lane secondary road that is 0.5 km long is at location  $x_{\text{ints}} = 0.5$  km; in mixed traffic flow, there are 1% of automated vehicles randomly distributed between human driving vehicles. Horizontal blue lines show road regions satisfying conditions (11) of [125] within which microscopic traffic situations have been used for the prediction. In simulations, the flow rate on the priority and secondary roads are, respectively, 1161 and 100 vehicles/h. Poisson distribution for entering vehicles has been used.

vehicle can merge on the priority road.

Thus, in the scenario under consideration without cooperative driving the automated vehicle cannot merge on the priority road without a stop at the intersection. For this reason the application of cooperative driving can have a sense. Simulations of the application of cooperative driving will be considered in Secs. IV A and V. Before the presentation of numerical simulation results, it is useful to give a *qualitative* explanation of the application of

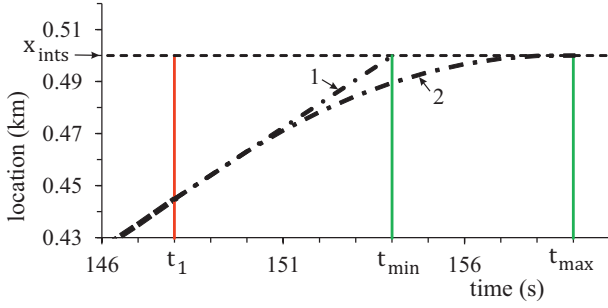


FIG. 4: Simulations of the prediction of time instants  $t_{\min}$  and  $t_{\max}$ . Calculations are made for prediction time instant  $t_p = t_1 = 148$  s: Virtual trajectories of the automated vehicle on the secondary road related to the prediction of  $t_{\min}$  (dashed-dotted curve 1) and to the prediction of  $t_{\max}$  (dashed-dotted curve 2), respectively. Other model parameters are the same as those in Fig. 3.

the general methodology for cooperative driving (Sec. II) for this case (Figs. 2(c, d)). First, in accordance of item (ii) of the general methodology, a cooperating vehicle is chosen (blue colored vehicle in Fig. 2(c)). The choice of this vehicle as the cooperating vehicle is as follows: From Fig. 2(b) we see that if this vehicle through its addition deceleration increases time headway  $\tau^-$  to the automated vehicle, then condition  $\tau^- \geq \tau_1$  can be satisfied. In this case, the automated vehicle can merge onto the priority road without stopping at the intersection. Second, in accordance of item (iii) of the general methodology, both motion requirements for the cooperating vehicle (like a required deceleration) and related characteristics of automated vehicle control are calculated with the use of the microscopic traffic prediction (Fig. 2(d)). Then, stages (ii) and (iii) of the general methodology explained in Figs. 2(c, d) for  $t_p = t_1$  are repeated at the next time instant  $t_{p+1}$ ,  $p = 1, 2, 3, \dots$ , when a next microscopic traffic situation is known, and so on. The prediction of the vehicle locations and vehicle speeds are used for the calculation of the future trajectory of the automated vehicle as well as all other vehicles involved in cooperative driving.

Before in Sec. V we consider simulation results of the scenario qualitatively explained in Fig. 2, we discuss how the cooperating vehicle is chosen in numerical simulations (Sec. IV A) as well as models of motion of the automated vehicle (Sec. IV B) and cooperative vehicle (Sec. IV C) based on microscopic traffic prediction.

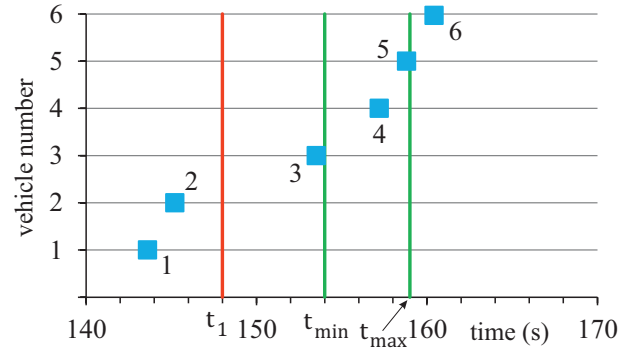


FIG. 5: Continuation of Fig. 3. Simulations of the prediction of time instants at which vehicles 1–6 moving on the priority road reach the intersection location  $x_{\text{ints}} = 0.5$  km. Numbers 1–6 are related to vehicles 1–6 in Fig. 3, respectively. Calculated predicted time instants at which locations of vehicles 3, 4, and 5 are at the intersection location  $x_{\text{ints}} = 0.5$  km are, respectively,  $t^{(3)} = 153.5$  s,  $t^{(4)} = 157.2$  s, and  $t^{(5)} = 158.8$  s.

## IV. CHARACTERISTICS OF COOPERATIVE DRIVING BASED ON MICROSCOPIC TRAFFIC PREDICTION

### A. Choice of Cooperating Vehicle based on Microscopic Traffic Prediction

At time instant  $t_1$ , based on the calculated microscopic traffic prediction (Fig. 3), a cooperating vehicle is found. We assume that all vehicles can communicate and are willing to cooperate with the automated vehicle. The choice of the cooperating vehicle is illustrated with Fig. 5.

We can see (Fig. 5) that time instant, at which location of vehicle 3 is at the intersection location  $x_{\text{ints}} = 0.5$  km, is slightly smaller than  $t = t_{\min}$ . Therefore, vehicle 3 can be chosen as the preceding vehicle for the automated vehicle merging onto the priority road without a stop at the intersection. Respectively, vehicle 4 that follows vehicle 3 can be chosen as the cooperating vehicle. The cooperating vehicle 4 should decelerate to ensure a safety merging of the automated vehicle onto the priority road without a stop at the intersection. This means that at time instant  $t = t_E$  the cooperating vehicle should be behind the automated vehicle at time gap  $\tau^- = \tau^{(c)}$  satisfying condition

$$\tau^{(c)} \geq \tau_1. \quad (8)$$

### B. Motion of Automated Vehicle in Cooperative Driving based on Microscopic Traffic Prediction

A required deceleration of the cooperating vehicle that satisfies condition (8) will be considered in Sec. IV C. Firstly, we should calculate deceleration  $b_p$  of the automated vehicle and related predicted time instant  $t = t_E$  at which the vehicle merges onto the priority road. Pre-



dicted time instant  $t = t_E$  is found from condition  $\tau^+ \geq \tau_2$  in (5) related to a safety merging of the automated vehicle behind of vehicle 3. The model of the calculation of the predicted time instant  $t_E$  and deceleration  $b_p$  of the automated vehicle is the same as that in Sec. III and Appendixes B and C of [125].

In accordance with [125], there is the repetition of the prediction of the automated vehicle trajectory made at each next time instants  $t_p$ ,  $p = 2, 3, \dots$ . Therefore, for each time instant  $t_p$ , the predicted time instant  $t_E$  and the associated predicted deceleration  $b_p$  are calculated. The automated vehicle motion with deceleration  $b_p$  is only valid until the next traffic prediction for  $b_{p+1}$  is calculated at  $t = t_{p+1}$ . In other words, deceleration  $b_p$  of the automated vehicle at time instant  $t_p$  is applied only during time interval (3). At  $t = t_{p+1}$ , the same procedure of microscopic traffic prediction as made for  $t = t_p$  is repeated leading to a new deceleration  $b_{p+1}$  and to a new predicted time instant  $t_E$  at which the vehicle should turn right onto the priority road. Then, during time interval  $t_{p+1} \leq t < t_{p+2}$  the vehicle moves in accordance with formulas (20) and (21) of [125] in which instead of the value  $b_p$  the new predicted deceleration  $b_{p+1}$  is used, and so on. Because microscopic traffic situations depend on time  $t_p$ , all predicted values, like the predicted time instant  $t_E(t_p)$ , are functions of time instant  $t_p$  at which the prediction is made.

In accordance with formula (2), time instants  $t_p$  at which the microscopic traffic prediction is made can be written as

$$t_p = t_1 + (p - 1)\tau, \quad p = 1, 2, \dots, p_E. \quad (9)$$

The repetition of the predictions of the automated vehicle trajectory is made up to some maximum time instant  $t_p$  denoted in (9) by  $t_p = t_{p_E}$ . Conditions for the maximum time instant  $t_p = t_{p_E}$  and for the related time instant denoted by  $t_E^{(\text{real})}$  at which the automated vehicle really merges onto the priority road are presented in Appendix C of [125]. At  $t \geq t_{p_E}$  the automated vehicle decelerates with the last predicted deceleration (Appendix C of [125]) moving up to the road intersection at which it turns right onto the priority road; later, no cooperating driving and no prediction is made.

### C. Motion of Cooperating Vehicle based on Microscopic Traffic Prediction

#### 1. Deceleration of Cooperating Vehicle

For each of the time instants  $t_p$ , the deceleration  $b_p^{(c)}$  of the cooperating vehicle that satisfies safety conditions (8) is found from condition:

$$x_{\text{ints}} - x_n^{(c)} = v_E^{(c)}\tau^{(c)} + d + X_b^{(c)}, \quad (10)$$

where index  $n$  corresponds to discrete time  $n\tau$ ,  $n = 0, 1, \dots$  of the model,  $x_n^{(c)}$  is the position of the coop-

erating vehicle at time  $t_n^{(c)}$ , where  $t_n^{(c)} = t_p$ ;  $v_E^{(c)} \geq 0$  is the calculated speed of the cooperating vehicle at time instant  $t_E(t_p)$ ,  $d$  is the vehicle length,  $X_b^{(c)}$  is a deceleration distance of the cooperating vehicle. The distance  $X_b^{(c)}$  and the speed  $v_E^{(c)}$  are found from the condition that the cooperating vehicle decelerates with constant deceleration  $b_p^{(c)} < 0$  from the speed  $v_n^{(c)}$  to the speed  $v_E^{(c)}$  during time interval  $T_c$ :

$$T_c(t_p) = t_E(t_p) - t_n^{(c)}, \quad (11)$$

$$X_b^{(c)} = v_n^{(c)} \left( T^{(c)} + \delta T^{(c)} \right) - \frac{1}{2} b_p^{(c)} T^{(c)} (T^{(c)} + \tau + 2\delta T^{(c)}), \quad (12)$$

$$v_E^{(c)} = \max \left( 0, v_n^{(c)} - b_p^{(c)} T^{(c)} \right), \quad (13)$$

where  $T^{(c)}$  and  $\delta T^{(c)}$  are, respectively, the integer and the fractional parts of time  $T_c$ :  $T^{(c)} = \tau \lfloor T_c / \tau \rfloor$ ,  $\delta T^{(c)} = T_c - T^{(c)}$ . Deceleration  $b_p^{(c)}$  is found from a solution of (10)–(13):

$$b_p^{(c)} = - \frac{2(x_{\text{ints}} - x_n^{(c)} - v_n^{(c)}(T^{(c)} + \delta T^{(c)} + \tau) - d)}{T^{(c)}(T^{(c)} + \tau + 2\delta T^{(c)} + 2\tau^{(c)})}, \quad (14)$$

where

$$p = 1, 2, \dots, p_E - 1. \quad (15)$$

The deceleration (14) is calculated for each time instant  $t_n^{(c)} = t_p$ . Then, under condition (15) the next prediction for the time  $t_E(t_{p+1})$  (see formula (31) of [125]) is made at time instant  $t_{p+1}$ , and the subsequent calculation of  $b_{p+1}^{(c)}$  is made.

#### 2. Minimum Distance for Cooperative Driving

At time instant  $t_n^{(c)}$  the cooperating vehicle is at some distance from the intersection location  $D = x_{\text{ints}} - x_n^{(c)}$ . It should be emphasized that there should be some minimum distance  $D = D_{\min}$  for cooperative driving; in other words, cooperative driving is possible when condition

$$D \geq D_{\min} \quad (16)$$

is satisfied. Indeed, first the deceleration of the cooperating vehicle is limited by a given maximum deceleration  $b_p^{(c)} = b_{\max}^{(c)}$ . In this case  $D_{\min} = D_{\min}^{(b)}$ , where

$$D_{\min}^{(b)} = d + v_n^{(c)} \left( T^{(c)} + \delta T^{(c)} + \tau^{(c)} \right) - \frac{1}{2} b_{\max}^{(c)} T^{(c)} \left( T^{(c)} + \tau + 2\delta T^{(c)} + 2\tau^{(c)} \right). \quad (17)$$

However,  $D_{\min}$  cannot exceed some value  $D_{\min}^{(0)}$ , because at the end of deceleration the final speed  $v_E^{(c)}$  in (13)



cannot be negative. Therefore, time  $T^{(c)}$  in (17) is limited by some value  $T_b^{(c)}$ . As a result,  $D_{\min}$  is equal to

$$D_{\min} = \begin{cases} D_{\min}^{(b)} & \text{at } T^{(c)} \leq T_b^{(c)} \\ D_{\min}^{(0)} & \text{at } T^{(c)} > T_b^{(c)}. \end{cases} \quad (18)$$

In order to find values of  $D_{\min}^{(0)}$  and  $T_b^{(c)}$  in (18), a case is considered when during some time steps  $N_b^{(c)}$  the cooperating vehicle decelerates with the maximum deceleration  $b_{\max}^{(c)}$  from the speed  $v_n^{(c)}$  to a very low speed  $v_c$  that satisfies conditions  $0 \leq v_c < b_{\max}^{(c)}\tau$ . Then,

$$N_b^{(c)} = \left\lfloor \frac{v_n^{(c)}}{b_{\max}^{(c)}\tau} \right\rfloor, \quad (19)$$

$$T_b^{(c)} = \tau N_b^{(c)}, \quad (20)$$

$$v_c = v_n^{(c)} - b_{\max}^{(c)}T_b^{(c)}. \quad (21)$$

From (21), value  $T_b^{(c)}$  can also be written as  $T_b^{(c)} = (v_n^{(c)} - v_c)/b_{\max}^{(c)}$ . At  $T^{(c)} = T_b^{(c)}$ , from Eq. (17) we get:

$$D_{\min}^{(0)} = d + \frac{1}{2}v_n^{(c)}(T_b^{(c)} - \tau) + \frac{1}{2}v_c(T_b^{(c)} + \tau + 2\delta T^{(c)} + 2\tau^{(c)}). \quad (22)$$

Using  $v_n^{(c)} = v_{\text{free}}$  (where  $v_{\text{free}}$  is a maximum vehicle speed) and condition  $v_c \ll v_{\text{free}}$ , formulas (20) and (22) read

$$T_b^{(c)} = \tau \left\lfloor \frac{v_{\text{free}}}{b_{\max}^{(c)}\tau} \right\rfloor, \quad (23)$$

$$D_{\min}^{(0)} = d + \frac{1}{2}v_{\text{free}}(T_b^{(c)} - \tau). \quad (24)$$

Eqs. (23) and (24) determine the parameters  $T_b^{(c)}$  and  $D_{\min}^{(0)}$  in formula (18) for  $D_{\min}$ .

Deceleration  $b_p^{(c)}$ ,  $p = 1, 2, \dots, p_E$  of the cooperating vehicle is found for each microscopic traffic prediction at time instants  $t_p$ . The calculated deceleration  $b_p^{(c)}$  can be different for different time instants  $t_p$ ,  $p = 1, 2, \dots, p_E$ .

## V. SIMULATION RESULTS OF COOPERATIVE DRIVING

At the beginning of microscopic traffic prediction  $t_1 = 148$  s, the following predictions have been calculated:

- (i) Time instant of automated vehicle merging  $t_E(t_1)$  onto the priority road behind vehicle 3.

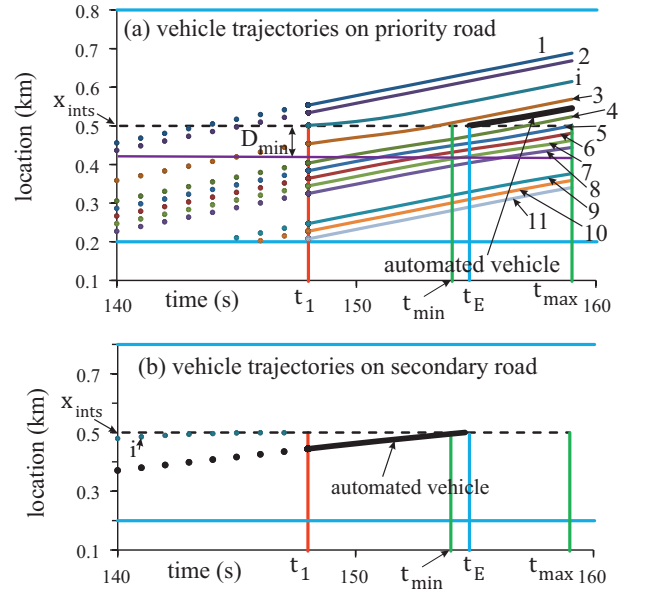


FIG. 6: Simulations of cooperative driving based on microscopic traffic prediction made for time instant  $t_1 = 148$  s: Trajectories of vehicles on the priority road (a) and secondary road (b). Dotted parts of vehicle trajectories are related to the microscopic traffic situation at  $t \leq t_1 = 148$  s, solid parts of vehicle trajectories are predicted vehicle trajectories. Model parameters:  $\tau^{(c)} = 2.4$  s,  $b_{\max}^{(c)} = 1$  m/s<sup>2</sup>. Calculated values  $t_{\min} = 154$  s,  $t_{\max} = 159$  s,  $t_E = 154.6$  s,  $\tau^- = 2.36$  s,  $\tau^+ = 0.97$  s,  $D_{\min} = 78.5$  m,  $T_c = 6.6$  s,  $b_1 = -0.21$  m/s<sup>2</sup>,  $b_1^{(c)} = -0.56$  m/s<sup>2</sup>. Other parameter designations, vehicle numbers, and model parameters are the same as those in Fig. 3.

- (ii) The deceleration of automated vehicle  $b_1$  (see Appendix C of [125]).
- (iii) A proof whether condition  $D \geq D_{\min}$  (16) is satisfied (Sec. IV C 2). If “Yes”, then next calculations of predicted characteristics (items (iv), (v)) are made.
- (iv) The deceleration of cooperating vehicle  $b_1^{(c)}$  (vehicle 4) (Sec. IV C).
- (v) The speeds and trajectories of all vehicles that locations correspond to conditions (11) of [125] (Figs. 6 and 7).

Calculations of the microscopic traffic prediction at the beginning of the prediction at time instant  $t_p = t_1$  are shown in Fig. 6. In this Fig. 6, dotted parts of vehicle trajectories are related to the microscopic traffic situation, whereas solid parts of vehicle trajectories are predicted vehicle trajectories. Time-functions of microscopic speeds of some of the vehicles of Fig. 6 are presented in Fig. 7. It should be emphasized that the prediction of values shown in Fig. 6 and listed in items (i)–(v) above, in particular,  $t_E(t_1)$ ,  $b_1$ , and  $b_1^{(c)}$  as well as of trajectories

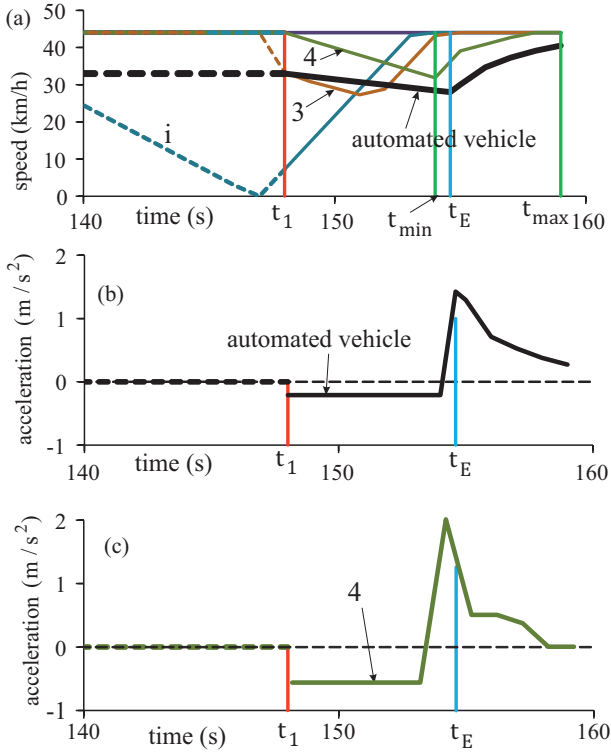


FIG. 7: Continuation of Fig. 6: (a) Time-functions of microscopic speeds of some of the vehicles; vehicles  $i$  and 3 are the preceding vehicles for the automated vehicle, respectively, on the secondary and priority roads. (b, c) Time-functions of deceleration (acceleration) of automated vehicle (b) and the cooperating vehicle (c). In (a, c), vehicle 4 is the cooperating vehicle. Vehicles numbers are the same as those in Fig. 6. Dashed parts of curves are related to real vehicle motion at  $t \leq t_1 = 148$  s, solid parts of curves are predicted characteristics.

of all vehicles have been calculated during a negligible short time interval  $\theta < 0.005$  s in comparison with time step  $\tau = 1$  s of the model. Corresponding to condition (3), the predicted values are used by the automated vehicle and cooperating vehicle during the time interval

$$t_1 \leq t < t_2. \quad (25)$$

At time instant  $t = t_2$ , the next microscopic traffic situation is available. Therefore, the next prediction of values  $t_E(t_2)$ ,  $b_2$ ,  $b_2^{(c)}$  as well as the new prediction of trajectories of all vehicles should be calculated and used for the motion of the automated vehicle and cooperating vehicle during the next time interval

$$t_2 \leq t < t_3, \quad (26)$$

and so on.

A dependence of predicted characteristics of the motion of the automated vehicle and cooperating vehicle on time instants  $t_p$ ,  $p = 2, 3, 4, 5, 6, 7$  is illustrated in Fig. 8. With the used of the microscopic traffic prediction, it has been found that at  $t_2 = 149$  s, to satisfy

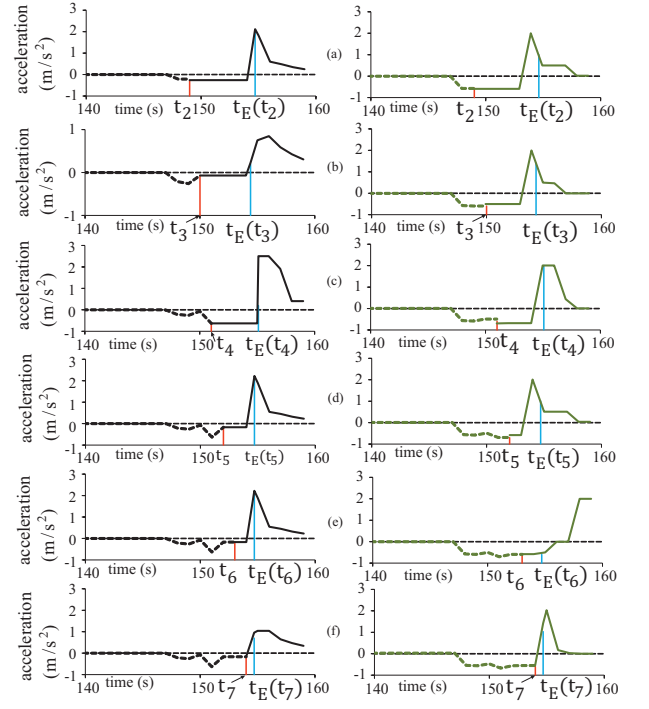


FIG. 8: Simulations of repetitions of prediction procedure for cooperating driving. Time-functions of deceleration (acceleration) of automated vehicle (left column) and the cooperating vehicle (right column) (vehicle 4 in Figs. 3, 6, and 7): (a)  $t_2 = 149$  s. (b)  $t_3 = 150$  s. (c)  $t_4 = 151$  s. (d)  $t_5 = 152$  s. (e)  $t_6 = 153$  s. (f)  $t_7 = 154$  s. Calculated predicted characteristics:  $t_E(t_2) = 154.7$  s,  $b_2 = -0.26$  m/s<sup>2</sup>,  $b_2^{(c)} = -0.59$  m/s<sup>2</sup> (a),  $t_E(t_3) = 154.4$  s,  $b_3 = -0.07$  m/s<sup>2</sup>,  $b_3^{(c)} = -0.5$  m/s<sup>2</sup> (b),  $t_E(t_4) = 155.1$  s,  $b_4 = -0.63$  m/s<sup>2</sup>,  $b_4^{(c)} = -0.7$  m/s<sup>2</sup> (c),  $t_E(t_5) = 154.7$  s,  $b_5 = -0.17$  m/s<sup>2</sup>,  $b_5^{(c)} = -0.59$  m/s<sup>2</sup> (d),  $t_E(t_6) = 154.7$  s,  $b_6 = -0.17$  m/s<sup>2</sup>,  $b_6^{(c)} = -0.59$  m/s<sup>2</sup> (e),  $t_E(t_7) = 154.7$  s,  $b_7 = -0.17$  m/s<sup>2</sup>,  $b_7^{(c)} = -0.58$  m/s<sup>2</sup> (f). Dashed parts of curves are related to real vehicle motion at  $t \leq t_p$ , where  $p = 2$  for (a),  $p = 3$  for (b),  $p = 4$  for (c),  $p = 5$  for (d),  $p = 6$  for (e), and  $p = 7$  for (f); solid parts of curves are predicted characteristics.

safety conditions (5), cooperating vehicle 4 should decelerate with  $b_2^{(c)} = -0.59$  m/s<sup>2</sup>; then, while decelerating with  $b_2 = -0.26$  m/s<sup>2</sup>, the automated vehicle can safe merge onto the priority road without stopping at the intersection at time instant  $t_E(t_2) = 154.7$  s (Fig. 8(a)). However, both the decelerations of the cooperating vehicle 4 and of the automated vehicle has been applied during the time interval  $t_2 \leq t < t_3$  only, where  $t_3 = 150$  s.

At  $t_3 = 150$  s, when a new microscopic traffic situation has been measured, through the use of new microscopic traffic prediction calculations of the decelerations of the cooperating vehicle 4 and of the automated vehicle as well as the predicted time instant of the automated vehicle merging  $t_E(t_3) = 154.4$  s have been made (Fig. 8(b)). However, both the decelerations of the cooperating vehicle

hicle 4 and of the automated vehicle have been applied during the time interval  $t_3 \leq t < t_4$  only, where  $t_4 = 151$  s. Calculations of the decelerations of the cooperating vehicle 4 and of the automated vehicle as well as the predicted time instant of the automated vehicle merging  $t_E$  have been repeated for further time instants  $t_3 = 151$  s,  $t_4 = 152$  s,  $t_5 = 153$  s, and  $t_6 = 154$  s, at which new microscopic traffic situations have been measured, respectively (Figs. 8(c–f)).

Thus, predicted decelerations  $b_p$  and  $b_p^{(c)}$  as well as other predicted characteristics of vehicle motion can be, respectively, different for different time instants  $t_p$ ,  $p = 2, 3, 4, 5, 6, 7$ . This explains why both the automated vehicle deceleration and the deceleration of the cooperating vehicle can be complex time functions within time interval  $t_1 \leq t < t_E^{(\text{real})}$  (Figs. 7–10).

To illustrate this conclusion, we compare the deceleration of cooperating vehicle 4 found from microscopic traffic predictions at time instants  $t_p$ ,  $p = 2, 3$ : Whereas at  $t_2 = 149$  s cooperating vehicle 4 decelerates with  $b_2^{(c)} = -0.59$  m/s<sup>2</sup>, at  $t_3 = 150$  s cooperating vehicle 4 should slightly reduce its deceleration to  $b_3^{(c)} = -0.5$  m/s<sup>2</sup>. The same effect is valid for the deceleration of the automated vehicle; for example, whereas at  $t_2 = 149$  s the automated vehicle should decelerate with  $b_2 = -0.26$  m/s<sup>2</sup>, however, at  $t_3 = 150$  s the automated vehicle should also reduce its deceleration to  $b_3 = -0.07$  m/s<sup>2</sup>.

In Figs. 9 and 10, simulations of cooperating driving based on *final* traffic prediction are presented. As explained in Sec. IV B, the final traffic prediction is made at time instant  $t_p = t_{pE}$  (9). At  $t \geq t_{pE}$ , the automated vehicle decelerates with the last predicted deceleration moving up to the road intersection at which it turns right onto the priority road. Later, no cooperating driving and no prediction is made, i.e., the automated vehicle moves on the priority road in accordance with rules of automated vehicle motion of [125].

Simulations of a speed harmonization in city traffic through the use of cooperative driving based on the microscopic traffic prediction are shown in Figs. 11 and 12. As can be seen from Fig. 11, the use of cooperative driving based on the microscopic traffic prediction leads to a speed harmonization in city traffic. However, the deceleration of the cooperating vehicle (vehicle 4) forces the following vehicles 5–8 also to decelerate (Fig. 12). Nevertheless, without cooperative driving the minimum speed of vehicles 4–8 is 33.5 km/h (Fig. 12(b)), whereas due to cooperative driving this minimum speed decreases only to 31.3 km/h (Fig. 12(a)). Thus, the decrease in the speed in vehicles following the automated vehicle caused by cooperative driving can be very low (in the case under consideration it is only 2.2 km/h) in comparison with a considerably larger effect of cooperative driving on the motion of the automated vehicle (Fig. 11).

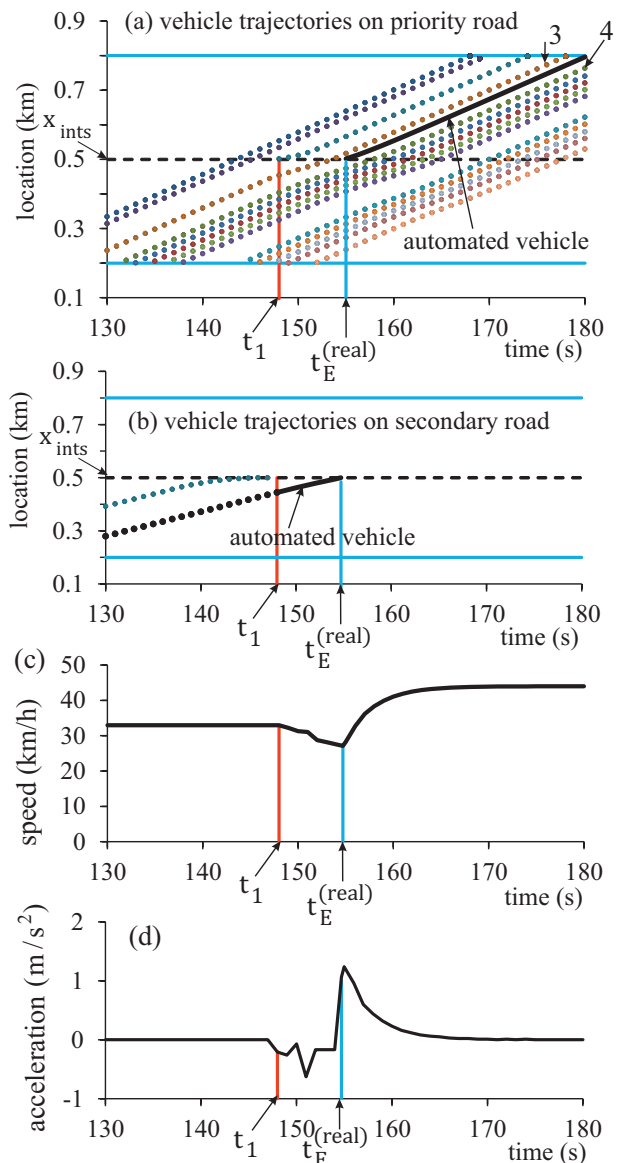


FIG. 9: Simulations of automated vehicle control through cooperating driving based on traffic prediction (final results): (a, b) Vehicle trajectories on the priority (a) and secondary roads (b); dotted curves are related to microscopic traffic situations, solid curves are motion of automated vehicle; in (a), vehicles 3 and 4 are, respectively, the preceding and cooperating vehicles. (c, d) Time-functions of speed (c) and deceleration (acceleration) of automated vehicle. Calculated value  $t_E^{(\text{real})} = 154.7$  s. Other parameter designations and model parameters are the same as those in Fig. 3.

## VI. DISCUSSION

### A. About Limitations of Cooperative Driving

As shown above, the use of cooperative driving based on the microscopic traffic prediction leads to a speed harmonization in city traffic. However, there is a consider-

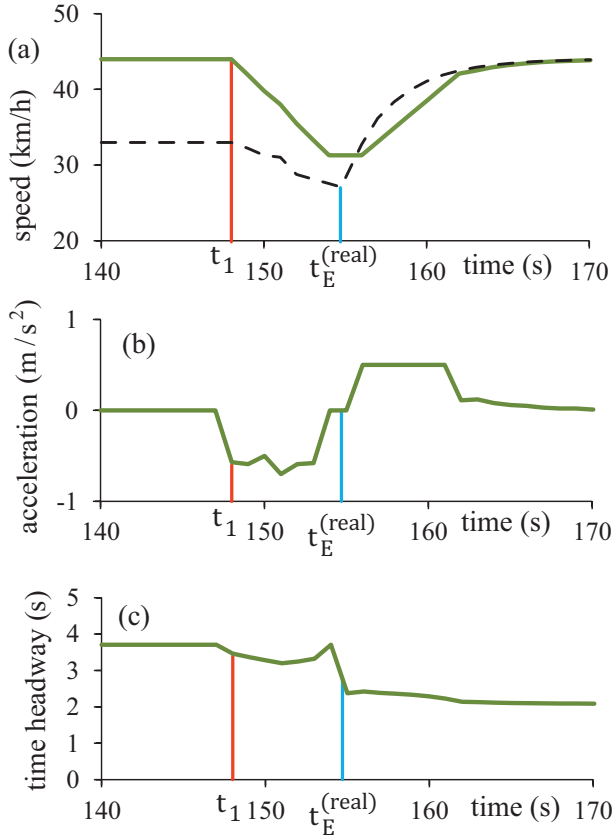


FIG. 10: Simulations of characteristics of motion of cooperating driving 4 based on traffic prediction (final results): Time-functions of speed (a), deceleration (acceleration) (b), and time headway of cooperating vehicle (c). In (a), dashed curve is time-dependence of automated vehicle speed taken from Fig. 9(c). Other parameter designations and model parameters are the same as those in Fig. 3.

able limitation of the applicability of cooperative driving.

To understand this limitation, we assume that vehicle 4 in Fig. 3 cannot cooperate or it does not want to cooperate. We assume that the next upstream vehicle 5 can cooperate and it wants to cooperate. We would like to understand in which degree the cooperation of vehicle 5 can improve traffic flow characteristics.

With this objective, we consider Figs. 5 and 13. Because we have assumed that vehicle 4 does not cooperate, the automated vehicle should merge onto the priority road behind vehicle 4. Therefore, the automated vehicle must decelerate before vehicle 4 is located already downstream of the intersection to satisfy safety condition  $\tau^+ \geq \tau_2$ . However, from Fig. 5 we can see that vehicle 4 reaches the intersection location  $x_{\text{ints}} = 0.5$  km at time instant  $t_{\text{cross}}^{(4)} = 157.2$  s (Fig. 13). At this time instant the automated vehicle speed is already equal to a very low value  $v_{\text{cross}}^{(\text{AV})} = 3.89$  km/h (Fig. 13). Thus, the automated vehicle can merge onto the priority road at some time instant  $t_E > t_{\text{cross}}^{(4)}$  while decelerating further to some lower

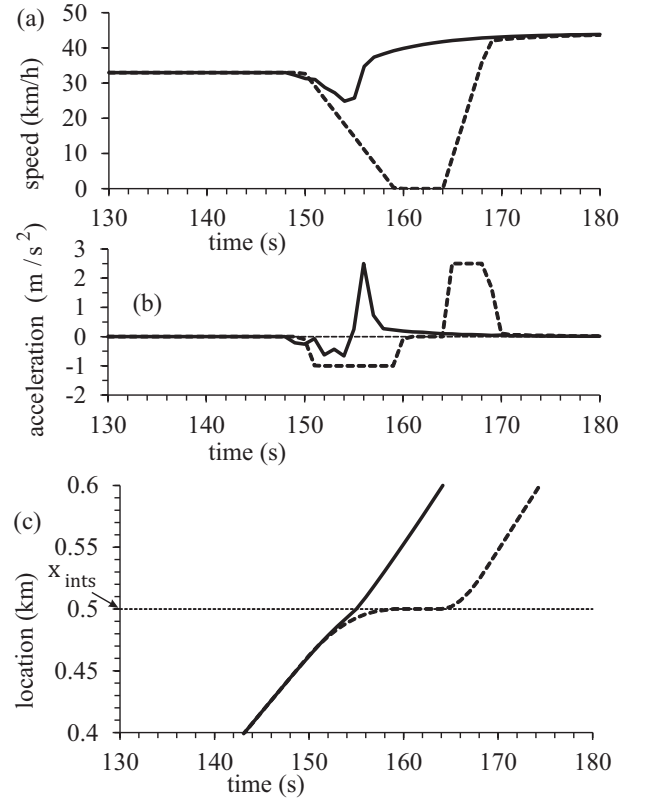


FIG. 11: Cooperative driving versus no cooperative driving: (a, b) Time-functions of speed (a) and deceleration (acceleration) (b) of the automated vehicle. (c) Trajectories of the automated vehicle. Solid curves – automated vehicle motion through cooperative driving; dashed curves – no cooperative driving is applied. Simulated data are taken from Fig. 3 for dashed curves and from Figs. 9 and 10 for solid curves.

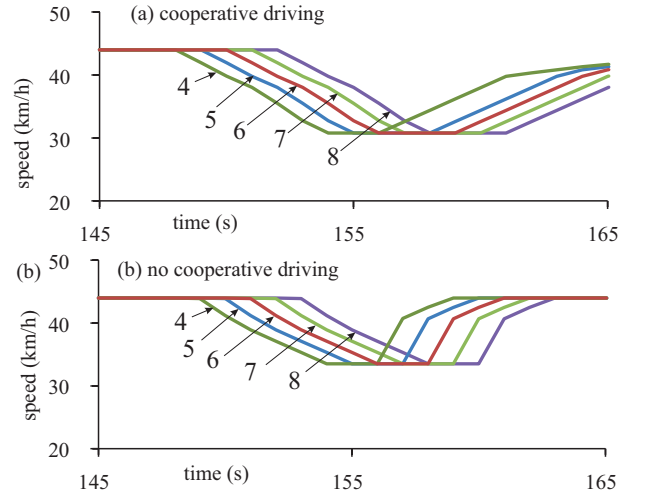


FIG. 12: Cooperative driving (a) versus no cooperative driving (b): Time-functions of some of the vehicles. Simulated data are taken from Figs. 9 and 10 for (a) and from Fig. 3 for (b). Vehicle numbers 4–8 are, respectively, the same as those in Fig. 3.

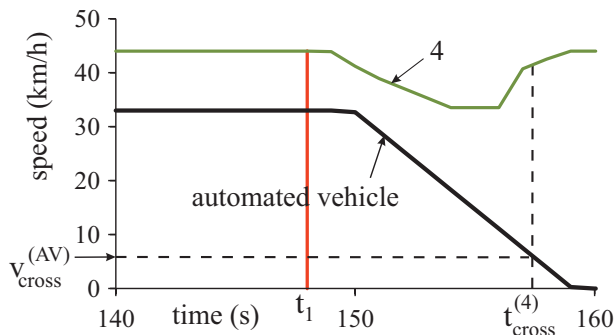


FIG. 13: Explanation of limitations of cooperative driving. Time-functions of speed of vehicle 4 and the automated vehicle along trajectories of these vehicles presented in Fig. 3. Calculated values:  $t_{\text{cross}}^{(4)} = 157.2$  s,  $v_{\text{cross}}^{(\text{AV})} = 3.89$  km/h.

speed  $v_E^{(\text{AV})} < 3.89$  km/h that is close to zero. Although even in this case of cooperative driving the automated vehicle can merge onto the main road without a stop at the intersection, it is realized on the cost of the deceleration of vehicle 5 and subsequent deceleration of some other following vehicles on the priority road. It seems that such cooperative driving is not effective enough to be used in the reality.

We see that even if in traffic flow only a few of the vehicles cannot cooperate or they do not want to cooperate, this can lead to considerable decrease in the effective use of cooperative driving. For this reason, a statistical analysis of cooperative driving based on microscopic traffic prediction for the case when some of the vehicles do not cooperate could be a very interesting task for further traffic studies. However, such a statistical analysis is a separate study, which is out of the scope of this paper. As above-mentioned (Sec. I), the objective of the paper is limited to the presented methodology of cooperative driving based on microscopic traffic prediction in mixed traffic flow with 100% of vehicles that participate in cooperative driving.

### B. Short-Time Prediction: Statistical Algorithms of Artificial Intelligence (AI) versus Microscopic Physical Traffic Modeling

Learning algorithms of AI are the important basis of many future technologies. This is also the case for future transportation technologies. In particular, as mentioned, in traffic science the short-time prediction of vehicle variables (vehicle locations and speeds) in the neighborhood of the automated vehicle, which is required for the planning of the trajectory of the automated vehicle, is made based on a diverse variety of statistical approaches of AI. Some of these statistical approaches have been mentioned above [72–124].

In the paper, rather than one of the statistical approaches of AI, we follow a qualitative different approach

to traffic prediction [125] in which no statistical analysis of a historical traffic database is used for traffic prediction. To explain our motivation, we should explain some basic physical traffic features. First, traffic occur in time and space. Second, vehicle locations and speeds are continuous time-variables. Third, traffic prediction needed for the confident planning of the trajectory of the automated vehicle can include a large enough number of vehicles whose locations and speeds should be predicted. Therefore, we can assume the following basic problems for applications of the statistical approaches of AI for the planning of the trajectory of the automated vehicle in real traffic:

- (i) For each part of a traffic network and even at the same initial traffic conditions at the network part boundaries, there can be *infinity number of microscopic traffic situations*. Therefore, a statistical database cannot include all possible microscopic traffic situations. This is true independent of the time duration within which traffic data included in this database have been measured.
- (ii) Because the statistical database cannot include all possible microscopic traffic situations (item (i)), in general case, the probability of the prediction of a particular microscopic traffic situation with a given high enough accuracy needed for *the safety planning* of automated vehicle trajectory is probably very difficult to determine.
- (iii) Due to differences in road infrastructure of different network parts within which the short-time prediction of vehicle variables in the neighborhood of the automated vehicle is made, it can occur that different historical traffic databases are needed for each of the network parts [151].

All these problems of the statistical approaches of AI for short-time microscopic traffic prediction in real traffic are absent in the approach to traffic prediction of [125]. This is because in this approach rather than statistical analysis of a historical traffic database, the microscopic modeling of the motion of each of the vehicles is used for microscopic traffic prediction. We see the following advantages of cooperative driving based on microscopic traffic prediction:

1. No statistical database for microscopic traffic prediction is needed.
2. A microscopic traffic flow model based on measured microscopic traffic situations (locations and speeds of vehicles) can predict future microscopic traffic situation. In accordance with this prediction, a decision for the motion of the cooperating vehicles and the safety planning of automated vehicle trajectory can be made.
3. Parameters of the microscopic traffic flow model can include a variety of vehicle behaviors adjustable



for different road infrastructure, like on- and off-ramps, road curves and road gradients etc. Therefore, in general there is no need to use different traffic models for each of the network parts.

It must be emphasize that statistical approaches of AI can also be very useful for the further development of the microscopic traffic prediction approach of [125]. Indeed, parameters of a microscopic traffic model used for the prediction can be automatically adapted over time with the use of learning approaches of AI. However, this task, which can be very interesting for further traffic studies, is out of the scope of this paper.

### C. Other Applications of Methodology for Cooperative Driving

We have illustrated and studied numerically the methodology of cooperative driving for a particular simple traffic scenario, in which a subject vehicle will to turn right at a unsignalized city intersection (Sec. III). From the stages of the methodology (Sec. II), it is clear that its applicability for other traffic scenarios is limited by the applicability of the microscopic traffic prediction of [125]. In a general case, the prediction of the motion of the local neighbors for the subject vehicle can depend on the behavior of the subject vehicle, whereas the behavior of the subject vehicle depends on the motion of the neighbor vehicles. In other words, without cooperative driving the microscopic traffic prediction can be applied at least when the predicted motion of the local neighboring vehicles does not depend on the subject vehicle motion. As explained in Sec. VII A of [125], there can be a number of other other possible applications of the microscopic traffic prediction in which these conditions are satisfied. Based on the prediction, cooperative vehicles and their behavioral parameters are chosen as explained in Sec. II.

As follows from Sec. II, the physical basis of the methodology for cooperative driving presented in the paper is the microscopic traffic prediction approach of [125]. Indeed, the prediction approach is used for all states of the application of cooperative driving that are as follows:

- (i) To make a decision whether cooperative driving is required for vehicle trajectory planning.
- (ii) To make a choice of required cooperative vehicles.
- (iii) To calculate the motion behaviors of the cooperative vehicles that satisfy driving safety conditions.

The microscopic traffic prediction approach of [125] used in the methodology of cooperative driving exhibits a general character. For this reason, the methodology of cooperative driving presented in this paper can be applied for different traffic scenarios in which the prediction approach is applicable. To explain these conclusions, below we consider qualitatively one of the traffic scenarios (Fig. 14).

Contrary to the simple scenario studied above, in which the automated vehicle tries to turn *right* at the

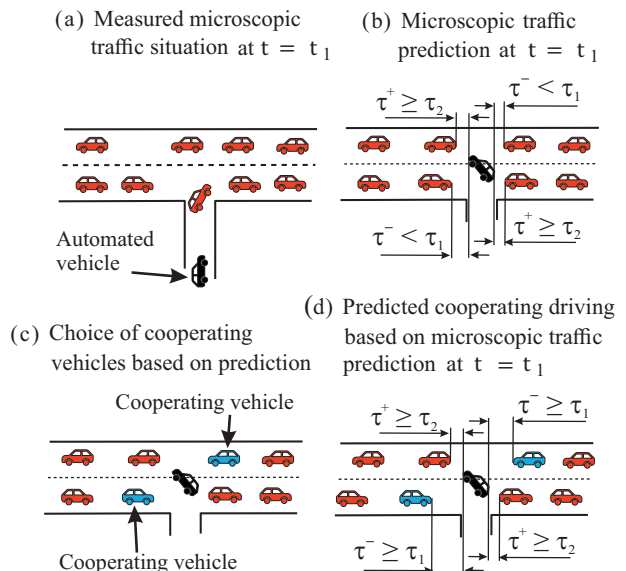


FIG. 14: Qualitative explanation of the application of the methodology for cooperative driving based on microscopic traffic prediction for a traffic scenario, in which a subject vehicle will to turn *left* at the unsignalized city intersection.

unsignalized intersection (Fig. 2), in the new considerably more complex scenario the automated vehicle tries to turn *left* at this intersection (Fig. 14).

In accordance with item (i) of the general methodology (Sec. II), we assume that in a traffic situation of this scenario (Fig. 14(a)) the application of microscopic traffic prediction without cooperative driving does not lead to the turning left of the automated vehicle onto the priority road without stopping at the intersection. This case is qualitatively shown in Fig. 14(b), in which the first of safety conditions (5) is not satisfied: Condition  $\tau^- < \tau_1$  is valid for both right and left traffic directions.

In accordance of item (ii) of the general methodology, cooperating vehicles are chosen (blue colored vehicles in Fig. 14(c)). The choice of these cooperating vehicles is as follows: From Fig. 14(b) we see that if these vehicles through their addition deceleration increase time headway  $\tau^-$  to the automated vehicle, respectively, in the right and left directions, then condition  $\tau^- \geq \tau_1$  can be satisfied for both directions. Therefore, the automated vehicle can merge onto the priority road without stopping at the intersection.

In accordance of item (iii) of the general methodology, motion requirements for the cooperating vehicles (like required decelerations) and related characteristics of automated vehicle control are calculated with the use of the microscopic traffic prediction (Fig. 14(d)). Then, stages (ii) and (iii) of the general methodology explained in Figs. 14(c, d) for  $t_p = t_1$  are repeated at the next time instant  $t_{p+1}$ ,  $p = 1, 2, 3, \dots$ , when a next microscopic traffic situation is known, and so on. The prediction of the vehicle locations and vehicle speeds are used for the

calculation of the future trajectory of the automated vehicle as well as all other vehicles involved in cooperative driving.

These qualitative conclusions should not be necessarily to be proven through numerical simulations of the traffic scenario shown in Fig. 14. This is due to the general character of the microscopic traffic prediction approach of [125] used for the methodology of cooperative driving of this paper. Indeed, the procedure of the prediction of values  $t = t_{\min}$ ,  $t = t_{\max}$ , and  $t = t_E$  in (4) for both potential pairs of vehicles moving in the right and left traffic directions on the priority road as well as the procedure of the calculation of requirements for the cooperating vehicles and automated vehicle control presented in [125] are general ones. This means that the microscopic prediction is independent of whether right or left traffic direction is considered. The difference of the scenario “left turning” (Fig. 14(b)) in comparison with the scenario “right turning” (Fig. 2(b)) is as follows: In Fig. 14, safety conditions (5) should be proven for *both* the right *and* left traffic directions[152].

Thus, due to a general character of the microscopic traffic prediction approach of [125], the methodology presented in the paper can be used for different traffic scenarios in which the prediction approach is applicable. For this reason, the physics of the methodology for cooperative driving could be understood from simulations of a simple scenario of right turning (Fig. 2) as made in the paper. Further simulations of the general methodology of cooperative driving for more complex scenarios can be very interesting for traffic engineering that are out of the scope of the paper.

#### D. Effect of Data Uncertainty on Prediction Reliability

Because measurements of microscopic traffic situations for unsignalized intersections are not available, microscopic traffic situations have been simulated with the same microscopic traffic flow model shortly discussed in Sec. I C. Moreover, we have assumed that vehicle speeds and locations in microscopic traffic situations that are used as initial conditions for the microscopic traffic prediction at time instants  $t_p$ ,  $p = 1, 2, \dots$  (see formula (22) of [125]) have no errors in comparison with real vehicle speeds and locations of microscopic traffic situations.

As shown in [147, 148], the Kerner-Klenov microscopic stochastic traffic flow model used in all simulations in this paper is able to simulate both microscopic and macroscopic measured (empirical) traffic data with a sufficient accuracy[153]. Nevertheless, the following question can arise: Is there a potential discrepancy between the predicted vehicle trajectories and the actual trajectories. Indeed, in reality there can be data latency errors and/or random errors in measurements of the vehicle speeds and locations in microscopic traffic situations used in the microscopic traffic prediction. We can call the errors the

uncertainty of traffic data used in the prediction model.

The related question how the robustness of the prediction model is maintained in the face of significant prediction errors caused by the uncertainty of traffic data has already been addressed in details in Secs. IV–VIII of [125]. It has been found that the microscopic traffic prediction can guarantee collision avoidance and safety traffic even when there is a considerable data uncertainty caused by data latency, random errors of the vehicle locations, and/or random errors of the vehicle speeds in the data of microscopic traffic situations. However, there is a critical uncertainty, i.e., the maximum amplitude of errors in the data of microscopic traffic situations at which the microscopic traffic prediction can still reliably be used for the automated vehicle control. There is probability  $P_{\text{app}}$  of the reliability of the application of the microscopic traffic prediction: when the data uncertainty does not exceed the critical uncertainty, then probability  $P_{\text{app}} = 1$  [125]. In this case, the microscopic traffic prediction is applicable for automated vehicle control.

#### E. Conclusions

1. We have introduced a methodology for cooperative driving in vehicular traffic based on time-limited microscopic traffic prediction that is performed based on the microscopic traffic modeling. Contrary to most approaches based on statistical algorithms of AI, no historical database is required for our approach.

2. With the use of microscopic traffic simulations of a simple city traffic scenario, we have proven the availability of the introduced methodology for the cooperative driving and studied its physical features.

3. Cooperative driving based on microscopic traffic prediction enables the control of the automated driving vehicle in mixed traffic in a complex city traffic scenario leading to a speed harmonization and, therefore, to increase in traffic comfort and safety in city traffic.

4. Due to a general character of the microscopic traffic prediction approach of [125], the methodology presented in the paper can be used for different traffic scenarios in which the prediction approach is applicable.

5. If the rate of communicating and cooperative vehicles in traffic flow becomes significantly less than 100%, the possibility of cooperative driving is likely to be very limited.

#### Acknowledgments

We thank our partners for their support in the project “LUKAS – Lokales Umfeldmodell für das Kooperative, Automatisierte Fahren in komplexen Verkehrssituationen” funded by the German Federal Ministry for Economic Affairs and Climate Action.



- 
- [1] R. Schmitz, M. Torrent-Moreno, H. Hartenstein, and W. Effelsberg, in 29th Annual IEEE International Conference on Local Computer Networks (IEEE, Tampa, Florida, USA, 2004), pp. 594–601.
- [2] J. Maurer, T. Fuegen, and W. Wiesbeck, in 11th European Wireless Conference 2005-Next Generation Wireless and Mobile Communications and Services (VDE-Verlag, Berlin, Germany, 2006), pp. 1–7.
- [3] Q. Chen, D. Jiang, V. Taliwal, and L. Delgrossi, in Proceedings of the 3rd International Workshop on Vehicular ad hoc Networks (VANET '06), (Association for Computing Machinery, New York, 2006), pp. 50–56.
- [4] T.-H. Wang, S. Manivasagam, M. Liang, B. Yang, W. Zeng, and R. Urtasun, in Computer Vision-ECCV 2020. ECCV 2020, Lecture Notes in Computer Science, Vol. 12347 edited by A. Vedaldi, H. Bischof, T. Brox, JM. Frahm. (Springer, Cham, 2020). [https://doi.org/10.1007/978-3-030-58536-5\\_36](https://doi.org/10.1007/978-3-030-58536-5_36)
- [5] Vehicular Communications and Networks, edited by W. Chen (Woodhead Publishing, Cambridge, 2015).
- [6] Automated Highway Systems, edited by P. A. Ioannou (Plenum Press, New York, 1997).
- [7] P. A. Ioannou and J. Sun, Robust Adaptive Control (Prentice Hall, Inc., Upper Saddle River, New Jersey, 1996).
- [8] P. A. Ioannou and C. C. Chien, IEEE Trans. Veh. Technol. 42 (1993) 657–672.
- [9] G. Meyer and S. Beiker, Road Vehicle Automation (Berlin, Springer, 2014).
- [10] C.-Y. Liang and H. Peng, JSME Jnt. J. Ser. C 43 (2000) 671–677.
- [11] L.C. Davis, Physica A 405 (2014) 128–139.
- [12] X. Chang, H. Li, J. Rong, X. Zhao, and A. Li, Physica A 557 (2020) 124829.
- [13] Y. Jiang, S. Wang, Z. Yao, B. Zhao, and Y. Wang, Physica A 582 (2021) 126262.
- [14] M. Papageorgiou, K.-S. Mountakis, I. Karafyllis, I. Pappachail and Y. Wang, Proceedings of the IEEE, 109 (2021) 114–121.
- [15] Z. Yao, Q. Gu, Y. Jiang, and B. Ran, Physica A 604 (2022) 127857.
- [16] Y. Jiang, S. Sun, F. Zhu, Y. Wu, and Z. Yao, Physica A 615 (2023) 128557.
- [17] K. Ma, H. Wang, and T. Ruan, Physica A 583 (2021) 126301.
- [18] R. Luo, Q. Gu, T. Xu, H. Hao, and Z. Yao, Physica A 597 (2022) 127211.
- [19] L. Ma, S. Qu, J. Ren, and X. Zhang, Mathematical Biosciences and Engineering 20 (2023) 2280–2295.
- [20] F. V. Monteiro and P. Ioannou, Transp. Res. C 151 (2023) 104138.
- [21] Weijie Yu, Dong Ngoduy, Xuedong Hua, Wei Wang, Transp. Res. C 157 (2023) 104389.
- [22] X. Li, Y. Xiao, X. Zhao, X. Ma, and X. Wang, Physica A 609 (2023) 128368.
- [23] Z. Gu, Z. Wang, Z. Liu, and M. Saberi, Transp. Res. C 138 (2022) 103626.
- [24] P. Hang, Y. Zhang, and C. Lv, IEEE Trans. ITS 24 (2023) 10420–10432.
- [25] Zhouzhou Yao, Xianyu Wu, Yang Yang, Ning Li, Physica A 633 (2024) 129365.
- [26] J. Shi, K. Li, C. Chen, W. Kong and Y. Luo, IEEE Trans. ITS 24 (2023) 11185–11197.
- [27] Baofeng Sun, Guodong Ma, Jia Song, Zeyang Cheng, Wei Wang, Physica A 630 (2023) 129215.
- [28] K. Hou, F. Zheng, X. Liu and G. Guo, IEEE Trans. ITS 24 (2023) 10774–10790.
- [29] Xin Huang, Huan Wang, Yongfu Li, Longwang Huang, Hang Zhao, Physica A 633 (2024) 129426.
- [30] Ying Shang, Feng Zhu, Rui Jiang, Xingang Li, Shupeii Wang, Transp. Res. C 158 (2024) 104441.
- [31] Keyi Liu, Tianjun Feng, Physica A 632 (2023) 129316.
- [32] Jiahua Qiu, Lili Du, Transp. Res. B 174 (2023) 102769.
- [33] N. Maiti, B.R. Chilukuri, Physica A 632 (2023) 129336.
- [34] L. An, X. Yang, D.-K. Kim, J. Hu, G. Wang, and Z. Xu, IEEE Trans. ITS 24 (2023) 10491–10500.
- [35] Zhentao Zhang, Xueyun Li, Chuqi Su, Xun Liu, Xin Xiong, Tianqi Xiao, Yiping Wang, Physica A 632 (2023) 129317.
- [36] Shu-Tong Wang, Wen-Xing Zhu, Xiao-Long Ma, Physica A 632 (2023) 129293.
- [37] Lihua Luo, Yi Liu, Yiheng Feng, Henry X. Liu, Ying-En Ge, Transp. Res. C 158 (2024) 104449.
- [38] Lin Hou, Yulong Pei, Qingling He, Physica A 632 (2023) 129307.
- [39] Ziyu Cui, Xiaoning Wang, Yusheng Ci, Changyun Yang, Jia Yao, Physica A 630 (2023) 129259.
- [40] Futao Zhang, Yongsheng Qian, Junwei Zeng, Dejie Xu, Haijun Li, Physica A 630 (2023) 129280.
- [41] Shi-Teng Zheng, Michail A. Makridis, Anastasios Kouvelas, Rui Jiang, Bin Jia, Transp. Res. C 152 (2023) 104151.
- [42] Leyi Duan, Yuguang Wei, Shixin Dong, Chen Li, Transp. Res. C 154 (2023) 104273.
- [43] Yangsheng Jiang, Hongwei Cong, Yi Wang, Yunxia Wu, Hongwu Li, Zhihong Yao, Physica A 630 (2023) 129289.
- [44] Ruijie Li, Siyuan Sun, Yunxia Wu, Huijun Hao, Xuguang Wen, Zhihong Yao, Physica A 627 (2023) 129130.
- [45] C. Liu, F. Zheng, R. Li and X. Liu, IEEE Trans. ITS 24 (2023) 15274–15287.
- [46] Dian Jing, Enjian Yao, Rongsheng Chen, Physica A 626 (2023) 129085.
- [47] X. Huang, P. Lin, M. Pei, B. Ran and M. Tan, IEEE Trans. ITS 24 (2023) 9501–9517.
- [48] Xia Li, Ziyi Liu, Mingye Li, Yimei Liu, Chunyang Wang, Xinwei Ma, Yaxin Liang, Physica A 625 (2023) 129040.
- [49] Jiawei Lu, Xuesong Simon Zhou, Transp. Res. C 153 (2023) 104223.
- [50] Yu Du, Michail A. Makridis, Chris M.J. Tampère, Anastasios Kouvelas, Wei ShangGuan, Transp. Res. C 156 (2023) 104319.
- [51] Yunjie Liu, Hao Wang, Changyin Dong, Yujia Chen, Physica A 624 (2023) 128934.
- [52] I. Gokasar, A. Timurogullari, S. S. Özkan, M. Deveci and Z. Lv, IEEE Trans. ITS 24 (2023) 13151–13160.
- [53] Jiawei Wang, Yingzhao Lian, Yuning Jiang, Qing Xu, Keqiang Li, Colin N. Jones, Transp. Res. C 155 (2023) 104274.
- [54] Jie Wang, Zhiyu Cai, Yaohui Chen, Peng Yang, Bokui Chen, Physica A 623 (2023) 128836.
- [55] Z. Huang, S. Shen and J. Ma, IEEE Trans. ITS 24

- (2023) 12754–12766.
- [56] Mengting Guo, Yang Bai, Xia Li, Wei Zhou, Chunyang Wang, Xinwei Ma, Huixin Gao, Yuewen Xiao, *Physica A* 623 (2023) 128894.
- [57] Qishen Zhou, Bin Zhou, Simon Hu, Claudio Roncoli, Yibing Wang, Jia Hu, Guangquan Lu, *Transp. Res. C* 156 (2023) 104320.
- [58] Yan-Tao Zhang, Mao-Bin Hu, Yu-Zhang Chen, Cong-Ling Shi, *Physica A* 623 (2023) 128828.
- [59] W. Yue, C. Li, S. Wang, N. Xue and J. Wu, *IEEE Trans. ITS 24* (2023) 12462–12476.
- [60] Chenguang Zhao, Huan Yu, Tamas G. Molnar, *Transp. Res. C* 154 (2023) 104230.
- [61] Minghao Fu, Shiwu Li, Mengzhu Guo, Zhifa Yang, Yaxing Sun, Chunxiang Qiu, Xin Wang, Xin Li, *Transp. Res. C* 157 (2023) 104415.
- [62] Cong Zhai, Ronghui Zhang, Tao Peng, Changfu Zong, Hongguo Xu, *Physica A* 623 (2023) 128903.
- [63] Yanyan Qin, Qinzhong Luo, Hua Wang, *Transp. Res. C* 157 (2023) 104370.
- [64] X. Duan, C. Sun, D. Tian, J. Zhou and D. Cao, *IEEE Trans. ITS 24* (2023) 7073–7091.
- [65] Z. Huang, H. Liu, J. Wu and C. Lv, *IEEE Trans. ITS 24* (2023) 7244–7258.
- [66] S. S. Mousavi, S. Bahrami and A. Kouvelas, *IEEE Trans. ITS 24* (2023) 6450–6462.
- [67] Weijie Yu, Xuedong Hua, Dong Ngoduy, Wei Wang, *Transp. Res. C* 154 (2023) 104265.
- [68] J. Wen, S. Wang, C. Wu, X. Xiao and N. Lyu, *IEEE Trans. ITS 24* (2023) 6463–6476.
- [69] A. Matin and H. Dia, *IEEE Trans. ITS 24* (2023) 2705–2736.
- [70] Milad Malekzadeh, Dimitrios Troullos, Ioannis Papatheodorou, Markos Papageorgiou, Klaus Bogenberger, *Transp. Res. C* 158 (2024) 104456.
- [71] Jun Ying, Yiheng Feng, *Transp. Res. C* 158 (2024) 104443.
- [72] S. Brechtel, T. Gindele, R. Dillmann, in *17th IEEE International Conference on Intelligent Transportation Systems, ITSC 2014*, 2014, pp. 392–399.
- [73] X. Lin, J. Zhang, J. Shang, Y. Wang, H. Yu, X. Zhang, in *2019 IEEE Intelligent Transportation Systems Conference, ITSC 2019*, 2019, pp. 2449–2455. doi:10.1109/ITSC.2019.8917348.
- [74] P. Schorner, L. Tottel, J. Doll, and J.M. Zollner, in *Proceedings of IEEE Intelligent Vehicles Symposium*, 2019, pp. 2299–2306. doi:10.1109/IVS.2019.8814022.
- [75] D. Klimenko, J. Song, H. Kurniawati, in *Australasian Conference on Robotics and Automation, ACRA*, 2014, Vol. 02-04-Dece.
- [76] P. Schorner, L. Tottel, J. Doll, and J.M. Zollner, in *Proceedings of IEEE Intel. Veh. Symposium*, 2019, pp. 2172–2179.
- [77] A. Lombard, A. Noubli, A. Abbas-Turki, N. Gaud and S. Galland, *IEEE Trans. ITS 24* (2023) 7178–7189.
- [78] J. Luo, T. Zhang, R. Hao, D. Li, C. Chen, Z. Na, Q. Zhang, *IEEE Trans. ITS 24* (2023) 5390–5405.
- [79] Xiaoyu Shi, Jian Zhang, Xia Jiang, Juan Chen, Wei Hao, Bo Wang, *Physica A* 633 (2024) 129353.
- [80] D. Isele, R. Rahimi, A. Cosgun, K. Subramanian, and K. Fujimura, in *Proceedings - IEEE International Conference on Robotics and Automation*, 2018, pp. 2034–2039, [1705.01196]. doi:10.1109/ICRA.2018.8461233.
- [81] Z. Qiao, K. Muelling, J. Dolan, P. Palanisamy, P. Mu-  
dalige, in *Proceedings of IEEE Conference on Intelligent Transportation Systems, ITSC*, 2018, Vol. 2018-Novem, pp. 2377–2382. doi:10.1109/ITSC.2018.8569400.
- [82] K. Sama, Y. Morales, H. Liu, N. Akai, A. Carballo, E. Takeuchi, K. Takeda, in *IEEE Transactions on Vehicular Technology*, 2020, pp. 1–1. doi:10.1109/tvt.2020.2980197.
- [83] D. Chen, M. R. Hajidavalloo, Zhaojian Li, K. Chen, Yongqiang Wang, Longsheng Jiang, and Yue Wang, *IEEE Trans. ITS 24* (2023) 11623–11638.
- [84] X. Jiang, J. Zhang, X. Shi and J. Cheng, *IEEE Trans. ITS 24* (2023) 5131–5143.
- [85] Changxi Ma, Mingxi Zhao, Xiaoting Huang, Yongpeng Zhao, *Physica A* 633 (2024) 129355.
- [86] W. Zhou, Z. Cao, N. Deng, K. Jiang and D. Yang, *IEEE Trans. ITS 24* (2023) 7932–7942.
- [87] J. Zhang, S. Li and L. Li, *IEEE Trans. ITS 24* (2023) 6280–6291.
- [88] Shupe Wang, Ziyang Wang, Rui Jiang, Feng Zhu, Ruidong Yan, Ying Shang, *Transp. Res. C* 158 (2024) 104445.
- [89] Renteng Yuan, Mohamed Abdel-Aty, Xin Gu, Ou Zheng, Qiaojun Xiang, *Physica A* 632 (2023) 129332.
- [90] G. Du, Y. Zou, X. Zhang, Z. Li and Q. Liu, *IEEE Trans. ITS 24* (2023) 8304–8323.
- [91] K. Guo, M. Wu, X. Li, H. Song and N. Kumar, *IEEE Trans. ITS 24* (2023) 10197–10210.
- [92] Chunyu Liu, Zihao Sheng, Sikai Chen, Haotian Shi, Bin Ran, *Physica A* 629 (2023) 129189.
- [93] J. Guo, L. Cheng and S. Wang, *IEEE Trans. ITS 24* (2023) 10501–10512.
- [94] Bharti, Poonam Redhu, Kranti Kumar, *Physica A* 625 (2023) 129001.
- [95] Wensong Zhang, Ronghan Yao, Xiaojing Du, Yang Liu, Rongyun Wang, Libing Wang, *Physica A* 625 (2023) 128988.
- [96] Shun Wang, Yong Zhang, Yongli Hu, Baocai Yin, *Physica A* 623 (2023) 128842.
- [97] Siyuan Feng, Shuqing Wei, Junbo Zhang, Yexin Li, Jintao Ke, Gaode Chen, Yu Zheng, Hai Yang, *Transp. Res. C* 156 (2023) 104331.
- [98] B. Li, Z. Huang, T.W. Chen, T. Dai, Y. Zang, W. Xie, B. Tian, K. Cai, *IEEE Trans. ITS 24* (2023) 8628–8637.
- [99] Jiaxin Liu, Rui Jiang, Jiandong Zhao, Wei Shen, *Transp. Res. C* 154 (2023) 104275.
- [100] Zelin Wang, Zhiyuan Liu, Qixiu Cheng, Ziyuan Gu, *Transp. Res. C* 158 (2024) 104439.
- [101] C. -J. Hoel, K. Wolff and L. Laine, *IEEE Trans. ITS 24* (2023) 6030–6041.
- [102] S. Fang, C. Zhang, S. Xiang and C. Pan, *IEEE Trans. ITS 24* (2023) 2827–2841.
- [103] P. F. Orzechowski, A. Meyer, M. Lauer, in *IEEE Conference on Intelligent Transportation Systems, ITSC (IEEE, Maui, Hawaii, USA, 2018)*, pp. 1729–1736.
- [104] M. Althoff S. Magdici, *IEEE Transactions on Intelligent Vehicles 1* (2016) 187–202.
- [105] M. Naumann, H. Konigshof, M. Lauer, and C. Stiller, in *Proceedings of IEEE Intelligent Vehicles Symposium (IEEE, Paris, France, 2019)*, pp. 140–145.
- [106] Ö. S. Tas, C. Stiller, in *Proceedings of IEEE Intelligent Vehicles Symposium*, 2018, pp. 1171–1178.
- [107] Y. Akagi and P. Raksincharoensak, in *Proceedings of IEEE Intelligent Vehicles Symposium (IEEE, Seoul, Ko-*

- rea, 2015), pp. 368–373.
- [108] Y. Morales, Y. Yoshihara, N. Akai, E. Takeuchi, and Y. Ninomiya, in Proceedings of IEEE Intelligent Vehicles Symposium (IEEE, Los Angeles, CA, USA, 2017), pp. 901–907.
- [109] Y. Morales, Y. Yoshihara, N. Akai, E. Takeuchi, and Y. Ninomiya, in IEEE International Conference on Intelligent Robots and Systems (IEEE, Vancouver, BC, Canada, 2017), pp. 3452–3459.
- [110] E. Takeuchi, Y. Yoshihara, and N. Yoshiki, in Proceedings of IEEE Conference on Intelligent Transportation Systems, ITSC (IEEE, Las Palmas, Spain, 2015), pp. 2311–2316.
- [111] M. Y. Yu, R. Vasudevan, and M. Johnson-Roberson, IEEE Rob. Autom. Lett. 4 (2019) 2235–2241.
- [112] S. Hoermann, F. Kunz, D. Nuss, S. Renter, K. Dietmayer, in Proceedings of IEEE Intelligent Vehicles Symposium (IEEE, Los Angeles, CA, USA, 2017), pp. 727–732.
- [113] Guojing Hu, Robert W. Whalin, Tor A. Kwembe, Weike Lu, Physica A 632 (2023) 129313.
- [114] Changxi Ma, Mingxi Zhao, Physica A 630 (2023) 129233.
- [115] S. Akhtar and S. Habibi, IEEE Trans. ITS 24 (2023) 9217–9239.
- [116] Xiaoxue Yang, Yajie Zou, Hao Zhang, Xiaobo Qu, Lei Chen, Physica A 624 (2023) 128912.
- [117] K. Gao, X. Li, B. Chen, L. Hu, J. Liu, R. Du, Y. Li, IEEE Trans. ITS 24 (2023) 6203–6216.
- [118] Ziqing Gu, Lingping Gao, Haitong Ma, Shengbo Eben Li, Sifa Zheng, Wei Jing, and Junbo Chen, IEEE Trans. ITS 24 (2023) 9966–9983.
- [119] Y. Zhang, W. Guo, J. Su, P. Lv and M. Xu, IEEE Trans. ITS 24 (2023) 9584–9598.
- [120] Xiaoyong Sun, Fenghao Chen, Yuchen Wang, Xuefen Lin, Weifeng Ma, Physica A 618 (2023) 128650.
- [121] Weibin Zhang, Huazhu Zha, Shuai Zhang, Lei Ma, Physica A 618 (2023) 128712.
- [122] H. Chen, Y. Liu, C. Hu and X. Zhang, IEEE Trans. ITS 24 (2023) 7306–7317.
- [123] W. Shao, Y. Xu, J. Li, C. Lv, W. Wang, and H. Wang, IEEE Trans. ITS 24 (2023) 11238–11253.
- [124] T. Qie, W. Wang, C. Yang, Y. Li, Y. Zhang, W. Liu, C. Xiang, IEEE Trans. ITS 24 (2023) 3999–4015.
- [125] B. S. Kerner and S. L. Klenov, Phys. Rev. E 106 (2022) 044307.
- [126] S. Dharba, K.R. Rajagopal, Transp. Res. C 7 (1999) 329–352.
- [127] A. Bose, P. Ioannou, Transp. Res. C 11 (2003) 439–462.
- [128] A. Kesting, M. Treiber, M. Schönhof, D. Helbing, Transp. Res. Rec 2000 (2007) 16–24.
- [129] A. Kesting, M. Treiber, M. Schönhof, D. Helbing, Transp. Res. C 16 (2008) 668–683.
- [130] A. Kesting, M. Treiber, and D. Helbing, Phil. Trans. Royal Society Series A 368 (2010) 4585–4605.
- [131] S. Kukuchi, N. Uno, M. Tanaka, Transp. Eng. 129 (2003) 146–154.
- [132] P. Y. Li, A. Shrivastava, Transp. Res. C 10 (2002) 275–301.
- [133] G. Marsden, M. McDonald, M. Brackstone, Transp. Res. C 9 (2001) 33–51.
- [134] J.-J. Martinez, C. Canudas-do-Wit, IEEE Trans. Control Syst. Technol. 15 (2007) 246–258.
- [135] S. E. Shladover, Veh. Syst. Dyn. 24 (1995) 551–595.
- [136] S. E. Shladover, D. Su, and X.-T. Lu, Transp. Res. Rec. 2324 (2012) 63–70.
- [137] A. Talebpour, H.S. Mahmassani, Transp. Res. C 71 (2016) 143–163.
- [138] B. S. Kerner, Phys. Rev. E 97 (2018) 042303.
- [139] B. S. Kerner, Physica A 562 (2021) 125315.
- [140] B.S. Kerner, *Breakdown in Traffic Networks: Fundamentals of Transportation Science* (Springer, Berlin, New York, 2017).
- [141] M. Takayasu, H. Takayasu, Fractals 1 (1993) 860–866.
- [142] A. Schadschneider, D. Chowdhury, K. Nishinari, *Stochastic Transport in Complex Systems*, (Elsevier Science Inc., New York, 2011).
- [143] P.G. Gipps, Trans. Res. B 15 (1981) 105–111.
- [144] S. Krauss, PhD thesis, DRL-Forschungsbericht 98-08 (1998) (available from [www.zaik.de/paper](http://www.zaik.de/paper)). <https://sumo.dlr.de/pdf/KraussDiss.pdf>
- [145] S. Krauss, P. Wagner, C. Gawron, Phys. Rev. E 55 (1997) 5597–5602.
- [146] W. Helly, in: Proceedings of the Symposium on Theory of Traffic Flow, pp. 207–238, Research Laboratories, General Motors, Elsevier, Amsterdam (1959).
- [147] B.S. Kerner, *The Physics of Traffic* (Springer, Berlin, New York 2004)
- [148] B.S. Kerner, *Introduction to Modern Traffic Flow Theory and Control*. (Springer, Berlin, New York, 2009).
- [149] It should be noted that in many publications devoted to a study of mixed traffic the analysis of the effect of automated driving on vehicular traffic is made (see, e.g., [126–139]). Contrary to such publications, in our paper *no* effect of automated vehicles on vehicular traffic is discussed. Instead, we apply the model of mixed traffic of Refs. [125, 138, 139] for simulations of cooperative driving based on the microscopic traffic prediction. We should also emphasize that in Refs. [125, 138, 139], in which the the model of mixed traffic used in the paper has been developed, the influence of automated vehicles and human-driving vehicle on mixed traffic as well as characteristics of automated vehicles have already been considered in details.
- [150] In simulations, in addition to this condition, to determine the beginning of the microscopic traffic prediction  $t_p = t_1$ , we have used the condition that the distance from the current automated vehicle location  $x^{(AV)}(t_p)$  to the location  $x_{\text{ints}}$  of the road intersection is less than some given value  $L_1$  (where  $L_1 = 0.15$  km), i.e.,  $x_{\text{ints}} - x^{(AV)}(t_p) < L_1$ . This condition is satisfied in all simulation results presented.
- [151] Examples of the differences in road infrastructure include different numbers of on- and off-ramps and distances between them, road gradients, road curves, changes in the number of road lanes, etc.
- [152] It can occurs that rather than the first of safety conditions (5) is not satisfied for both right and left traffic directions (Fig. 14(b)), this safety condition is not satisfied only for one of the directions. Then, only one cooperating vehicle should be chosen for the traffic direction for which the first of safety conditions (5) is not satisfied.
- [153] See also references to origin papers cited in the books [147, 148] about the empirical proof of the Kerner-Klenov microscopic stochastic traffic flow model.